https://rbgeomorfologia.org.br/
ISSN 2236-5664

Revista Brasileira de Geomorfologia

v. 25, nº 4 (2024)

http://dx.doi.org/10.20502/rbgeomorfologia.v25i4.2584

Research Article

Landslide susceptibility mapping using logistic regression, random forests, and artificial neural networks: a case study in Mariana/MG, Brazil

Mapeamento da Suscetibilidade a deslizamentos utilizando regressão logística, florestas aleatórias e redes neurais artificiais: estudo de caso em Mariana/MG, Brasil

Mateus Oliveira Xavier [1] and César Falcão Barella [2]

[1] Federal University of Ouro Preto, Architecture and Urbanism Department, Ouro Preto, Brazil. mateus.xavier@ufop.edu.br. ORCID: https://orcid.org/0000-0002-3441-8208

[2] Federal University of Ouro Preto, Environmental Engineering Department, Ouro Preto, Brazil. cesarbarella@ufop.edu.br. ORCID: https://orcid.org/0000-0001-6005-9125

Received: 08/05/2024; Accepted: 30/09/2024; Published: 05/11/2024

Abstract: The landslide susceptibility mapping (LSM) plays an important role in risk management. This study evaluated the predictive capabilities of three machine learning (ML) approaches applied to LSM: logistic regression (LR), random forests (RF), and artificial neural networks (ANN). The study was conducted in a mountainous region of Mariana/MG, Brazil. Initially, a point inventory with 364 landslides and 364 stable regions was randomly partitioned in a 70% training and 30% testing ratio for the models. Nine landslide conditioning factors (LCF), ranked by information gain (IG), were considered: slope angle (IG=0.486), geomorphology (IG=0.235), topographic wetness index - TWI (IG=0.138), lithology (IG=0.077), slope orientation (IG=0.067), topographic position index - TPI (IG=0.052), distance from drainage (IG=0.032), slope curvature (IG=0.029) and the distance from roads (IG=0.024). The evaluation of the area under the curve (AUC-ROC) and the classification efficiency rates in high ($ER_{\mathrm{i}}^{\mathrm{HS}}$) and low ($ER_{\mathrm{i}}^{\mathrm{LS}}$) susceptibility were used to compare the results of the approaches. The results demonstrated that although RF (AUC-ROC=0,947, $\mathrm{ER}_{\mathrm{i}}^{\mathrm{HS}}$=6,808, $\mathrm{ER}_{\mathrm{i}}^{\mathrm{LS}}$=0,030) slightly outperformed LR (AUC-ROC=0,936, $\mathrm{ER}_{\mathrm{i}}^{\mathrm{HS}}$=5,695, $\mathrm{ER}_{\mathrm{i}}^{\mathrm{LS}}$=0,050) and ANN (AUC-ROC=0,934, $\mathrm{ER}_{\mathrm{i}}^{\mathrm{HS}}$=6,495, $\mathrm{ER}_{\mathrm{i}}^{\mathrm{LS}}$=0,060), all the approaches exhibited high predictive capability in identifying areas susceptible to landslides.

Keywords: Machine learning; Predictive analysis; Landslide conditioning factors; Risk management.

Resumo: O mapeamento da suscetibilidade a deslizamentos (MSD) desempenha importante papel na gestão de riscos. Este estudo avaliou as capacidades preditivas de três abordagens de aprendizado de máquina (ML) aplicadas ao MSD: regressão logística (RL), florestas aleatórias (FA) e redes neurais artificiais (RNA). O estudo foi realizado em uma localidade montanhosa de Mariana/MG, Brasil. Inicialmente, um inventário pontual com 364 deslizamentos e 364 regiões estáveis foi particionado aleatoriamente na proporção de 70% para treinamento e 30% para testagem dos modelos. Nove fatores condicionantes aos deslizamentos (FCD), hierarquizados pelo ganho de informação (GI), foram considerados: declividade (GI=0,486), geomorfologia (GI=0,235), índice topográfico de umidade - TWI (GI=0,138), litologia (GI=0,077), orientação das vertentes (GI=0,067), índice de posição topográfica - TPI (GI=0,052), distância da rede de drenagem (GI=0,032), curvatura das vertentes (GI=0,029), distância das vias (GI=0,024). A avaliação da área abaixo da curva (AUC-ROC) e das taxas de eficiência da classificação na alta (TE_i^{AS}) e na baixa (TE_i^{BS}) suscetibilidade foram utilizadas para comparar os resultados das abordagens. Os resultados demonstraram que, embora FA (AUC-ROC=0,947, TE_i^{AS}=6,808, TE_i^{BS}=0,030) tenha resultados ligeiramente melhores que RL (AUC-ROC=0,936, TE_i^{AS}=5,695, TE_i^{BS}=0,050) e RNA (AUC-ROC=0,934, TE_i^{AS}=6,495, TE_i^{BS}=0,060), todas abordagens demonstraram alta capacidade preditiva em identificar áreas suscetíveis a deslizamentos.

Palavras-chave: Aprendizado de máquina; Análise preditiva; Fatores condicionantes aos deslizamentos; Gestão de riscos.

1. Introduction

Landslides are among the most recurrent geodynamic events worldwide, causing extensive environmental damage and significant socioeconomic losses annually (CHEN; YU; LI, 2018; HUANG; LI, 2011; TANOLI et al., 2023; TZOUVARAS, 2021). In the context of Latin America and the Caribbean, Brazil had the highest number of recorded landslides with fatalities between 2004 and 2013 (SEPÚLVEDA; PETLEY, 2015). Most of these incidents are associated with intense rainfall concentrated during the summer months, particularly in mountainous areas with steep slopes (AHRENDT; ZUQUETTE, 2003; HIRYE et al., 2023; TIAGO DAMAS et al., 2017).

Uncontrolled urban expansion in areas susceptible to geodynamic processes, coupled with the low construction standards of buildings and the lack of adequate public housing policies, emerge as key factors contributing to the high damage caused by landslides in Brazil. Therefore, it is of utmost importance that these areas have access to tools that consider landslide susceptibility, as well as risk and hazard assessments, to ensure efficient and safe land use as well as land cover management (FELL et al., 2008). In this context, landslide susceptibility maps are fundamental elements for the prevention and mitigation of landslide impacts, assisting planners, local administrators, and decision-makers in land use and land cover planning (KAVZOGLU; SAHIN; COLKESEN, 2014).

Landslide susceptibility mapping (LSM) is a graphical assessment methodology that estimates the spatial probability of these events based on the local characteristics of the investigated region (ALEOTTI; CHOWDHURY, 1999; FELL et al., 2008). Since the 1970s, numerous methodologies have been developed for this purpose (KAVZOGLU; TEKE, 2022; MAURIZIO; MARIA, 2012), which are usually classified into (ALEOTTI; CHOWDHURY, 1999; SOETERS; VAN WESTEN, 1996; YOUSSEF; POURGHASEMI, 2021): (I) direct geomorphological mapping (e.g. CARVALHO et al., 2013; SOBREIRA et al., 2013; ZIMMERMANN; BICHSEL; KIENHOLZ, 1986), where through expert interpretation, susceptibility classes are defined directly in the field, providing a simple and straightforward approach, but on the other hand, being highly subjective and dependent on the experience of the experts (GUZZETTI et al., 1999; SOETERS; VAN WESTEN, 1996); (II) heuristic methods (e.g. BLAIS-STEVENS; BEHNIA, 2016; ELMOULAT et al., 2021; RUFF; CZURDA, 2008; STANLEY; KIRSCHBAUM, 2017), where the developed maps result from the prioritization and weighting of landslide-triggering processes through map algebra, with the final outcome linked to the relevance assigned to each of these processes (FERNANDES et al., 2001; TSAI et al., 2013); (III) deterministic physically-based approaches (e.g. ARMAŞ et al., 2014; DO PINHO; AUGUSTO FILHO, 2022; JOVANČEVIC et al., 2018; MICHEL; KOBIYAMA; GOERL, 2014), based on the physical and mathematical relationships that define slope stability, correlating geometric data with geotechnical resistance parameters through simulations that integrate hydrological and slope stability models. Although they provide robust results, the complexity of obtaining and spatializing geotechnical parameters may limit the application of these models to smaller and more homogeneous areas (ALEOTTI; CHOWDHURY, 1999; YILMAZ, 2009); (IV) data-driven statistical methods, which estimate susceptibility based on the statistical relationship between landslide inventories and their conditioning factors, where susceptibility is estimated by identifying patterns in the spatial distribution of past landslides, systematically relating these records to the conditioning factors adopted by the models to predict new occurrences (CHACÓN et al., 2006; GUZZETTI et al., 1999; REICHENBACH et al., 2018).

Various statistical approaches, including bivariate, multivariate, and more recently, machine learning techniques, have been applied in LSM in different parts of the world (e.g. ALEOTTI; CHOWDHURY, 1999; CALDERÓN-GUEVARA et al., 2022; COCO et al., 2021; EIRAS et al., 2021; MURILLO-GARCÍA; ALCÁNTARA-AYALA, 2015; NOHANI et al., 2019; PIMIENTO, 2010; PRADHAN; SEENI; KALANTAR, 2017; SANTACANA et al., 2003; SOETERS; VAN WESTEN, 1996). Some of the most commonly used statistical methodologies include the likelihood ratio, information value, weights of evidence, favorability functions, discriminant analysis, logistic regression (LR), random forests (RF), and artificial neural networks (ANN) (COROMINAS et al., 2014).

In this context, as noted by Barella, Sobreira, and Zêzere (2019), different LSM approaches have already been compared by various authors (e.g. AKGUN, 2012; CHEN et al., 2023; LIU et al., 2022; MERGHADI et al., 2020; PHAM et al., 2016; WANG et al., 2021; YOUSSEF; POURGHASEMI, 2021). Comparisons are important for identifying the advantages and limitations of each method, allowing researchers to select the most suitable approaches for the characteristics and specificities of the investigated regions, thus contributing to the advancement of methodologies and promoting the development of increasingly robust and refined approaches.

In recent years, publications addressing evaluations and comparisons between statistical machine learning (ML) methods for LSM have gained prominence (e.g. JENNIFER, 2022; LIU et al., 2022; OLIVEIRA et al., 2019; YI et al., 2019). Some of the advantages of these methods include objective statistical grounding, reproducibility, the ability for continuous updating, capacity to handle extensive datasets, and robust results (SIDUMO; SONONO; TAKAIDZA, 2022; YOUSSEF; POURGHASEMI, 2021).

In this study, we conducted the training, evaluation, and comparison of three statistical ML techniques – RF, LR and ANN – to create landslide susceptibility maps in a mountainous region of Minas Gerais, located in southeastern Brazil. For this purpose, and for each technique used, we selected, sampled, classified, and filtered nine factors that influence landslides. The sampling was carried out through a landslide inventory and stable areas constructed via photointerpretation and fieldwork. At the end of the study, we assessed the validation rate of the susceptibility maps produced by the best model of each technique. Thus, the objective of this research focused on determining whether the chosen ML techniques are appropriate for modeling and mapping landslide susceptibility in the investigated region.

2. Study Area

The study area, illustrated in Figure 1 by the colored composition from the Sentinel-2 satellite on April 28, 2020, is located in the southeastern portion of the Doce River Basin and southeast of the Mariana municipality, historically known as the first capital in the state of Minas Gerais, Brazil. Geographically, it extends between latitudes 20°22'S and 20°26'S, and longitudes 43°13'W and 43°18'W, encompassing, to the northwest, the rural district of Cachoeira do Brumado.

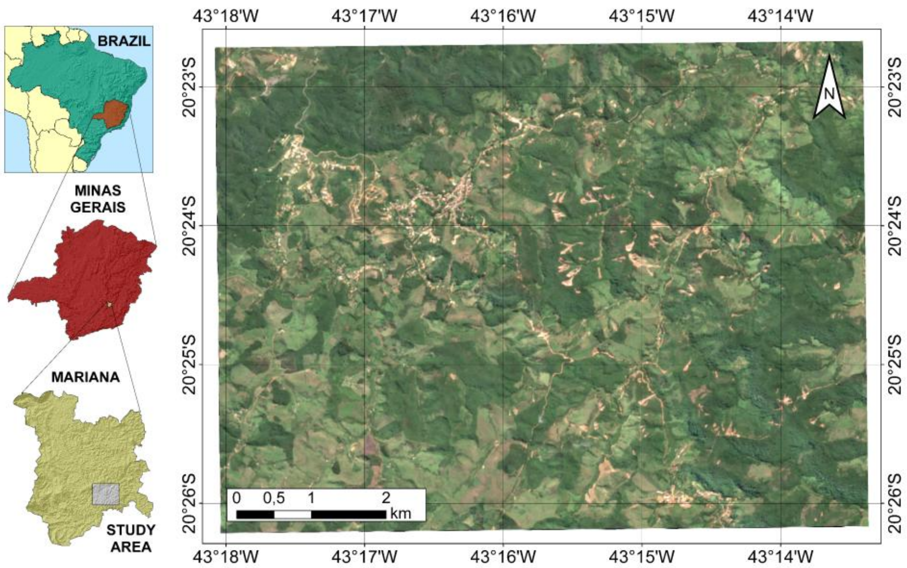

Figure 1. Color composition from the Sentinel-2 satellite for the study area on April 28, 2020

The climate is predominantly humid, with an average annual temperature of approximately 20°C and peak precipitation occurring during the summer months (SOUZA et al., 2006). According to the National Center for Monitoring and Natural Disaster Alerts (CEMADEN, 2024), the region has experienced intense rainfall, particularly in the first quarter of 2020, when heavy precipitation resulted from the influence of the South Atlantic Convergence Zone and the passage of cold fronts over the Doce River Basin (LOTT et al., 2021). As a consequence, a total of 191 mm of rainfall was recorded between February 6 and 13, with a peak of 51.6 mm occurring in the early hours of February 13. This event triggered 364 simultaneous and predominantly translational landslides, with volumes ranging from 11 to 68235 m^3, which were identified through photointerpretation and fieldwork.

Geologically, the area is composed of lateritic soils derived from gneissic rocks, with transitions in vegetation cover between the Cerrado and Atlantic Forest, featuring a diversity of grasses, cyperaceae, pastures, and forests of varying heights (BATISTA, 2006; SOUZA, 2004). The relief is predominantly mountainous, with regions exhibiting steep slopes and significant elevation changes. Altitudes range from 486 to 938 meters above sea level, with an average slope of approximately 21° and a maximum of 68°. Finally, the study area is close to a dense network of natural drainage, including the Cachoeira do Brumado Stream. During intense rainfall events, this hydrographic network contributes to soil saturation, which is a significant triggering factor for landslides in the region.

3. Materials and Methods

This article presents and compares three ML approaches to produce landslide susceptibility maps. The processing, training, and testing of the models were conducted using Orange Data Mining 3.34.0 (DEMSAR et al., 2013), while spatial data manipulation was conducted in a QGIS 3.12.3-București (QGIS DEVELOPMENT TEAM, 2020). The SIRGAS2000 Datum was adopted in all geoprocessing stages. The data utilized included information collected from fieldwork, satellite images, a geological map at a scale of 1:25,000, and a topographic map at a scale of 1:10,000. The methodology adopted in the study is illustrated in Figure 2.

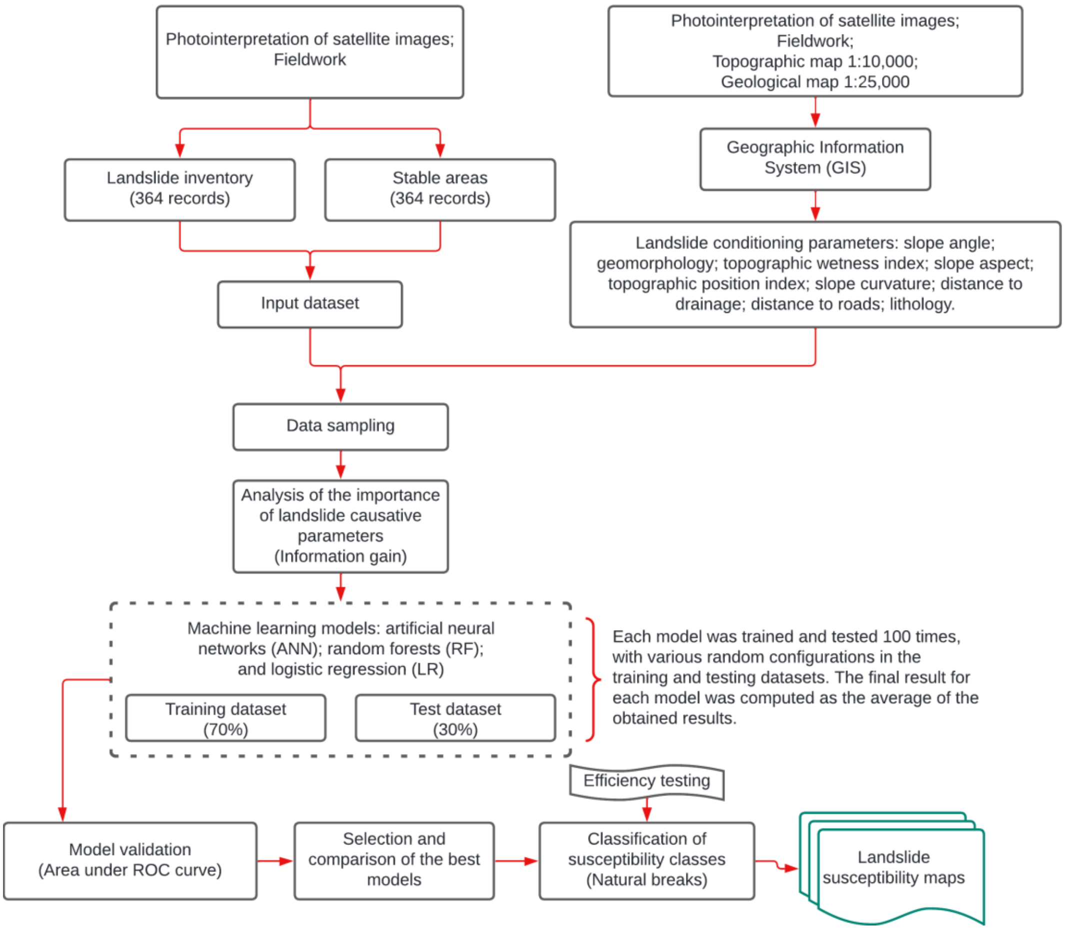

Figure 2. Flowchart of the study presenting the adopted methodology

3.1. Landslides and stable areas inventory

In order to model landslide susceptibility using ML techniques, it is necessary to have an input dataset that includes records of past landslides and areas considered stable (without landslides). This dataset should sample the landslide conditioning factors (LCF) for the training and testing of the models (BORGA et al., 1998). In this context, we assume that new events are likely to occur in areas with characteristics similar to those of previously affected regions (ALEOTTI; CHOWDHURY, 1999; FELL et al., 2008; GUZZETTI et al., 1999).

The development of landslide inventories can be conducted through a variety of techniques, ranging from fieldwork and historical record research to the photointerpretation of aerial images (GALLI et al., 2008; GUZZETTI et al., 2000). These methodologies can be applied either in isolation or in combination, providing an integrated approach to identifying landslides. Thus, through fieldwork and photointerpretation of satellite images, we constructed an inventory with 364 landslides points and 364 representative points of stable areas within the study area (Figure 3). To identify these regions, we used a color composition of the visible spectrum bands (red, green, and blue), Bottom-of-Atmosphere (BOA) level, from the Sentinel-2 mission of the European Space Agency (ESA), acquired on April 28, 2020, with cloud coverage below 4.8% and 10 m spatial resolution. Additionally, we visually verified some smaller landslides identified in the field using Google Earth Pro and Microsoft Bing Maps platform, which provide a spatial resolution of less than 1 m. For the construction of the inventory, we placed a point vector at the failure zone of each of the 364 identified landslide features. Subsequently, we randomly distributed 364 points in the remaining areas of the study region to represent the stable areas.

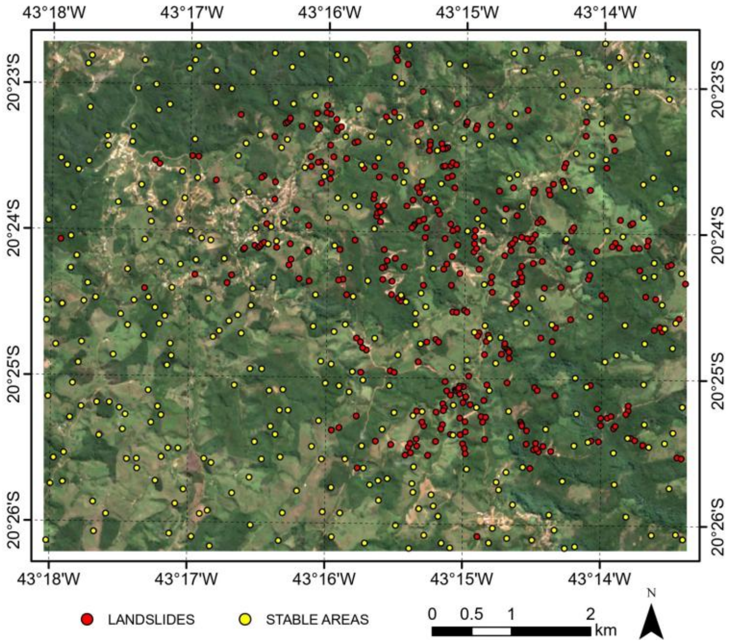

Figure 3. Landslides and stable areas inventory

Finally, with the dependent variables defined in a 1:1 ratio (unstable: stable), the input dataset was divided into a subgroup for model construction (training) and another for result validation (testing). There is no standard predefined categorization for modeling landslide susceptibility (YOUSSEF; POURGHASEMI, 2021). In the literature, a common division of 70% for training and 30% for testing is often adopted (e.g. DAO et al., 2020; PHAM et al., 2016; SHAHABI et al., 2023), which was also utilized in this work. This procedure represents the most commonly used data partitioning technique in data-driven landslide susceptibility models (LIMA et al., 2022). In order to ensure robustness, we repeated this training and testing division 100 times for each model, obtaining the final results by validating all individual outcomes from the simulated iterations.

3.2. Landslide Conditioning Factors (LCF)

The selection of LCF for modeling susceptibility is of utmost importance, as it can directly impact the accuracy and reliability of the results. Although there is no specific guideline for this selection, it is crucial that the chosen LCF are representative of the characteristics of the study area and the landslides in question (CHEN; POURGHASEMI; NAGHIBI, 2018; XU et al., 2013). Furthermore, it is essential that these factors have an analysis scale compatible with the research objectives (SHIRANI; PASANDI; ARABAMERI, 2018). In our study, we opted for nine LCF (Figure 4), of which seven were extracted from the digital terrain model (DTM) derived from a topographic map at a scale of 1:10,000, covering slope angle, geomorphology, topographic wetness index (TWI), slope aspect, topographic position index (TPI), slope curvature, and distance from the natural drainage network. The distance from roads was derived from the photointerpretation of satellite images and fieldwork. Finally, the lithology at a scale of 1:25,000 was obtained from geological maps produced by Endo et al. (2019) and Pinheiro, Magalhães, and Silva (2023). Except for the slope curvature, which was prepared at a spatial resolution of 30 m x 30 m, all other LCF were prepared at a resolution of 10 m x 10 m.

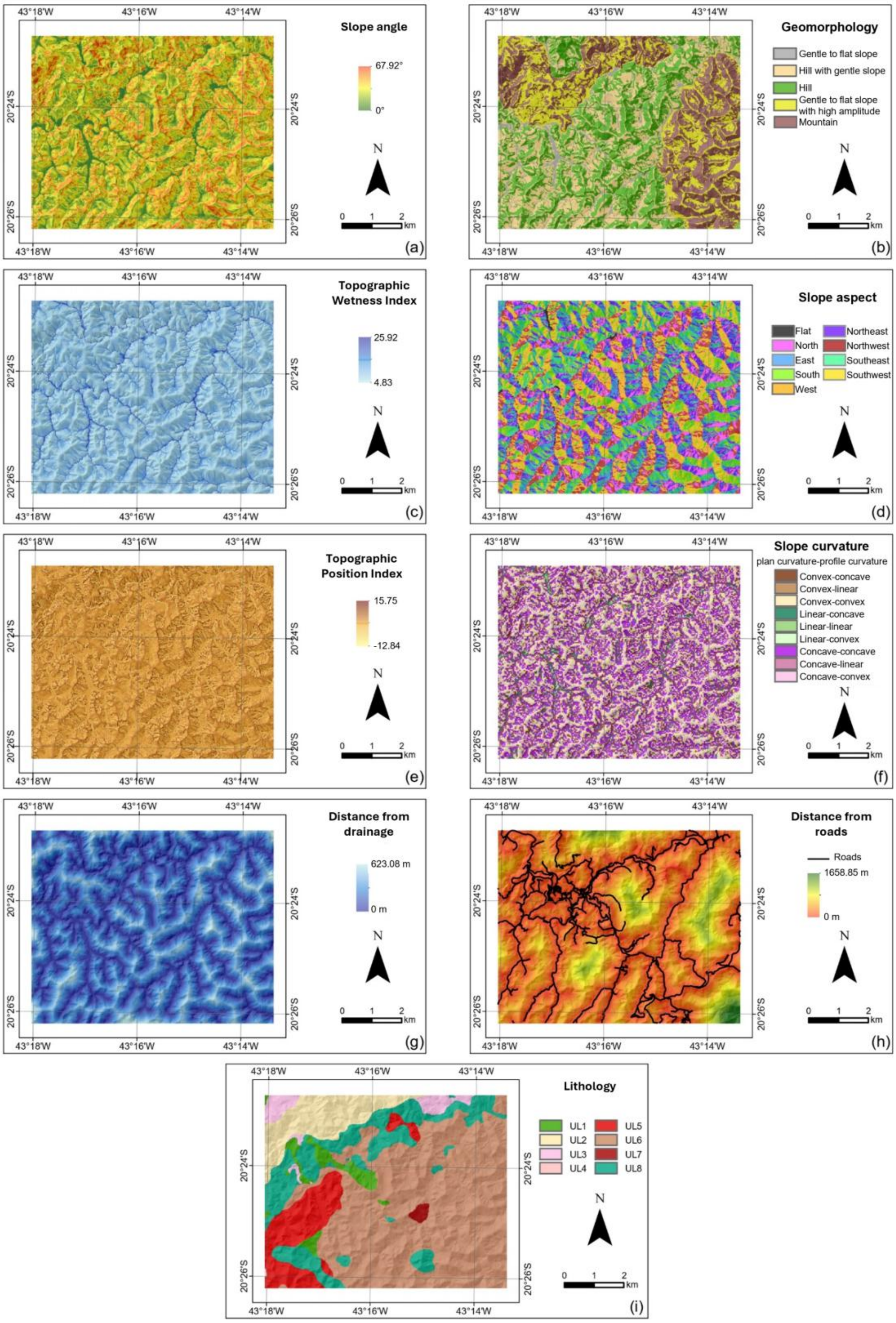

Figure 4. Landslide conditioning factors: (a) slope angle, (b) geomorphology, (c) Topographic Wetness Index (TWI), (d) slope aspect, (e) Topographic Position Index (TPI), (f) slope curvature, (g) distance from drainage, (h) distance from roads, and (i) lithology.

3.2.1. Slope angle

In slope stability and LSM, slope angle is one of the first factors to be considered due to its direct influence on shear strength, one of the physical fundamentals for triggering mass movements (LEE; MIN, 2001; OGILA, 2021).

According to Guillard and Zezere (2012), the instability of soils and rocks tends to increase as the slope angle increases. In our study, the adopted slope map covers inclinations are ranging from 0° to 67.92° (Figure 4a).

3.2.2. Geomorphology

Geomorphology can reveal the geological processes that shaped the terrain in the past, thus providing important clues about areas more prone to landslides. This is because different landform configurations exert varying influences on the likelihood of such events occurring (ANBAZHAGAN; SAJINKUMAR, 2011). The geomorphological units of the study area, shown in Figure 4b, were classified based on predominant slope angle (expressed as a percentage) and local amplitude (the elevation difference between the base and top of terrain units defined by the inverted DTM), following the methodology proposed by Souza (2015); Souza and Sobreira (2017), as presented in Table 1. Five geomorphological classes were established for the study area: gentle to flat slope, hill with gentle slope, hill, gentle to flat slope with high amplitude, and mountain.

Table 1. Classification of geomorphological units (Souza, 2015; Souza and Sobreira, 2017)

Local amplitude (m)	Predominant slope angle	Relief class
< 100	< 5%	Gentle to flat slope with low amplitude
	5 a 10%	Ramp
	10 a 20%	Knoll
	> 20%	Hillock
100 a 300	< 5%	Gentle to flat slope*
	5 a 20%	Hill with gentle slope*
	> 20%	Hill*
> 300	< 20%	Gentle to flat slope with high amplitude*
	> 20%	Mountain*

* Geomorphological classes identified in the study area

3.2.3. Topographic Wetness Index (TWI)

The TWI assesses the degree of moisture at a given location based on topography (POURGHASEMI et al., 2012; YESILNACAR; SÜZEN, 2006). In areas where water accumulation is significant, soil saturation tends to increase during rainy periods, which can raise the likelihood of landslides in locations with higher index values (JEBUR; PRADHAN; TEHRANY, 2015; NEFESLIOGLU; DUMAN; DURMAZ, 2008). This occurs due to a decrease in cohesion among soil grains, resulting in reduced shear strength. The index is established from Equation 1, proposed by Moore, Grayson and Ladson (1991):

$$\mathrm{TWI} = ln\left(\frac{\mathrm{A}}{tg(\beta)}\right) \tag{1}$$

Where:

- A is the specific contributing area of the local watershed (m^2/m)
- β is the local slope angle (in degrees)

For the study area, the TWI values ranged from 4.83 to 25.92, with higher values indicating a greater tendency for water accumulation, as observed in Figure 4c.

3.2.4. Slope aspect

The slope aspect is an important factor to consider in LSM (CHEN; NIU; JIA, 2016; GUZZETTI et al., 2005). The direction in which a slope is oriented controls certain microclimatic aspects, which can directly or indirectly influence the occurrence of landslides, such as solar exposure, wind direction, rainfall intensity, soil moisture, and vegetation development (CONFORTI et al., 2014; EIRAS et al., 2021). For the study area, the slope aspect, shown in Figure 4d, was classified into nine classes according to the azimuth angle of the slopes: flat (without azimuth indication), north (0°-22.5°; 337.5°-360°), northeast (22.5°-67.5°), east (67.5°-112.5°), southeast (112.5°-157.5°), south (157.5°-202.5°), southwest (202.5°-247.5°), west (247.5°-292.5°), and northwest (292.5°-337.5°).

3.2.5. Topographic Position Index (TPI)

The TPI shows the difference between the elevation of a point and the average elevation of its surroundings (ESLAMINEZHAD; EFTEKHARI; AKBARI, 2020; PAWLUSZEK; BORKOWSKI, 2017). The consideration of TPI in LSM arises from the argument that such events typically occur at the ridges of the slopes (BACHRI et al., 2019; EFIONG et al., 2021), where TPI exhibits positive values, indicating lower elevations in the surrounding areas. However, the negative TPI values suggest the opposite, indicating that the areas around the analyzed point have higher elevations (LEE; LEE; LEE, 2018). In the study area, TPI values ranged from -12.84 to 15.75, as illustrated in Figure 4e.

3.2.6. Slope curvature

According to Ullah et al. (2022), a slope can exhibit three distinct types of curvature in each of its planes, both vertical (profile curvature) and horizontal (plan curvature): convex, concave, and flat. Profile curvature is responsible for determining the dynamics of water flow acceleration along the slope, influencing the processes of erosion and debris deposition. Slopes with concave profile curvature tend to be more prone to landslides (GRABOWSKI et al., 2022; OHLMACHER, 2007). On the other hand, plan curvature influences the convergence and divergence of water flows. Areas with concave or convergent plan curvature tend to be more susceptible to landslides (GRABOWSKI et al., 2022).

In the present study, plan curvatures were combined with profile curvatures in nine different combinations (DIKAU, 1990). For better visual acuity of the curvatures and to avoid unwanted effects of the DTM on the final result, the resulting map, shown in Figure 4f, was created at a spatial resolution of 30 m x 30 m (GARCIA, 2012).

3.2.7. Distance from natural drainage

Hydrological conditions play an important role in triggering landslides (THANH; DE SMEDT, 2012). For this reason, several authors have employed the distance to the drainage network as a LCF (BISWAS; RAHAMAN; BARMAN, 2023; BISWAS; RANJAN, 2021; OH; LEE, 2011), given the tendency for some landslides to occur near the drainage. Thus, the distance to the drainage network was considered in our study in an ordinal manner, ranging from 0 m to 623.08 m, as shown in Figure 4g.

3.2.8. Distance from roads

Some authors hypothesize that landslides are more likely to occur near roads or pathways, primarily due to the geometric alteration of slopes (cuts and fills) and the interference with natural drainage (ABU EL-MAGD; ALI; PHAM, 2021; DAHAL et al., 2008). This hypothesis was reinforced during fieldwork in the study area, where several landslide scars were identified close to the roads. The distance to the map of the roads, represented in Figure 4h, was developed in an ordinal manner, covering distances that ranged from 0 m to 1658.85 m for the study area.

3.2.9. Lithology

Lithological variations are an important parameter for geological risk analyses and LSM (HENRIQUES; ZÊZERE; MARQUES, 2015; POURGHASEMI; KERLE, 2016; RAHMATI et al., 2016). Physical, hydrological, and mechanical characteristics, such as strength, density, permeability, and weathering degree, vary according to lithological type (NAEMITABAR; ZANGANEH ASADI, 2021; YOUSSEF; POURGHASEMI, 2021). For the study area, eight lithological units were extracted at a scale of 1:25,000, as shown in Table 2 and Figure 4i, based on the work of Endo et al. (2019) and Pinheiro, Magalhães, and Silva (2023).

Table 2. Characterization of the lithological units present in the study area

Code	Lithology
UL1	Metamafic rocks: amphibolites, amphibole schists, and mylonites
UL2	Meta-sandstones and impure meta-arkoses
UL3	Migmatites: metatexites and gneisses
UL4	Clayey-sandy sediments: mudstones with fine arenaceous-siltstone levels
UL5	Biotite metagranites, granodiorites, and tonalites
UL6	Paleoproterozoic injection gneisses over migmatites and Archean gneisses, mafic, and meta-ultramafic rocks
UL7	Banded iron formation
UL8	Meta-ultramafic rocks: soapstones, serpentinites, schists, and mylonites

3.3. Landslide conditioning factors (LCF) ranking

In the context of ML models for susceptibility mapping, the ranking of LCF serves as an important preprocessing step. This phase aims to evaluate the impact of conditioning factors on the accuracy and reliability of the models (SAHIN et al., 2020). The objective is to eliminate superfluous or redundant information, while establishing the optimal combinations of factors (PHAM et al., 2021).

In our study, we ranked the LCF using Information Gain (IG), a highly effective technique for selecting influential variables, which is widely adopted in the ML field (LI et al., 2022; QUINLAN, 1986). According to Pham et al. (2017), IG is quantified based on the measure of entropy reduction in the LCF and it offers a valuable approach for evaluating their contribution to the landslide susceptibility modeling.

In this context, the nine LCF considered in the study were hierarchically ranked based on IG, where higher values indicate a more significant contribution of the factor to the model construction.

3.4. Selection of machine learning technique for the landslide susceptibility modeling

We evaluated the performance of three ML approaches for landslide susceptibility modeling: RF, LR, and ANN. The number of LCF considered in each learning technique varied from 4 to 9, with integration based on the ranking produced by Information Gain (IG). Initially, only the four attributes with the highest IG values were included, gradually expanding to cover all available LCF. Our analysis focused on the best-performing model developed for each set with the same number of LCF. In other words, for each approach, we evaluated and compared the best model using 4, 5, 6, 7, 8, and 9 LCF.

3.4.1. Random Forests (RF)

RF is a non-parametric ensemble learning classification method developed by Breiman (2001). The input data is arbitrarily selected and resampled in equal proportions into smaller subsets known as decision trees, using the bagging technique (CRUZ; OLIVEIRA, 2021; UEHARA et al., 2020), where the final classification is determined by the most frequent result among the created subsets. In order to build the model, the user must define the number of trees in the forest and the number of attributes to be considered at each tree node. The nodes represent decision points where data is split based on certain criteria. Each node may have zero or more branches, representing different paths in the decision-making process. These procedures allow for the creation of trees with relatively low bias and high variance, therefore, contributing to a better model performance (HASTIE; TIBSHIRANI; FRIEDMAN, 2009; PHAM et al., 2019; ZHANG et al., 2017).

In this study, various models were developed, hence exploring a wide range of configurations. These variations included different numbers of trees, ranging from 10 to 100, with increments of 10 trees at each step. Additionally, the number of LCF considered at each tree node ranged from two, thus representing the minimum number possible, to the maximum number of LCF available in each model.

3.4.2. Logistic Regression (LR)

LR, introduced by Cox (1958), and Walker and Duncan (1967), is a multivariate analysis approach used to model the probability of a characteristic or outcome (LEE, 2004, 2005). The approach estimates the binary probability of a dependent variable using a logistic function, which allows a linear combination of independent predictor variables to be transformed into a value that can be interpreted as a probability (MASCANZONI et al., 2018). Over the years, LR has become the most widely used statistical method for LSM worldwide due to its simplicity and effectiveness (CHOWDHURY, 2023; DOMÍNGUEZ-CUESTA et al., 2010; POURGHASEMI et al., 2018).

In order to mitigate overfitting and enhance the generalization ability of LR models, regularization techniques are commonly employed, particularly Lasso (L1) and Ridge (L2) methods (ABDELRAHMAN, 2020; NG, 2004). While L1 regularization can zero out some regression coefficients, removing less relevant variables, L2 reduces overfitting by decreasing the impact of highly correlated variable coefficients without necessarily excluding them (KOPPE; MEYER-LINDENBERG; DURSTEWITZ, 2021; MIRANDA; BOMBACINI, 2023). The intensity of regularization is influenced by the cost parameter C, where a lower value implies stronger regularization and a higher value reduces this strength.

Various LR configurations were tested, varying the regularization methods between L1 and L2 and adjusting the cost parameter C from 0.001 to 1000.

3.4.3. Artificial Neural Networks (ANN)

ANN, introduced by McCulloch and Pitts (1943), is a supervised learning classification technique inspired by the neural structure of the human brain. They are designed to recognize patterns and learn from input data through a training process (AGATONOVIC-KUSTRIN; BERESFORD, 2000; MOULOODI et al., 2021). In our study, we utilized a multi-layer perceptron (MLP) ANN with a backpropagation algorithm. The MLP operates by feeding the data into an input layer, which is then processed through one or more hidden layers of neurons. These basic computational units mimic the functioning of biological neurons in the human brain, utilizing weights and activation functions (ALALOUL; QURESHI, 2020; PARK; LEK, 2016). The correction and optimization of weights occur through the backpropagation method, which adjusts the weights based on the error between the predicted output and the actual output. This iterative process allows the MLP to learn complex patterns in the data, making it a powerful tool for analyzing and modeling complex systems (GARDNER; DORLING, 1998; NASKATH; SIVAKAMASUNDARI; BEGUM, 2023; ZAJMI; AHMED; JAHARADAK, 2018).

For the activation function, we chose the Rectified Linear Unit (ReLU) function (NAIR; HINTON, 2010; XU et al., 2015). This choice was due to its recognized simplicity and computational efficiency, along with its widespread use in training ANN (NOLA, 2022; PAUL et al., 2023). To adjust the weights of the neurons and minimize the prediction error of the ANN, we adopted the Adam optimizer, using the Adaptive Moment Estimation method (KINGMA; BA, 2014). The Adam optimizer was selected due to its efficiency and the strong performance demonstrated in ML studies focused on landslides (e.g. NHU et al., 2020; PANDEY et al., 2022; WANG et al., 2020; YI et al., 2022).

In order to reduce the risk of overfitting and to maintain the construction of simpler models, we opted to use a single hidden layer of neurons in the ANN. The number of neurons in each developed model was determined based on the maximum value established by Equation 2, proposed by Hecht-Nielsen (1987), which considers both the number of neurons in the hidden layer (H) and the number of LCF employed in the model (n).

$$H \leq 2n + 1 \quad (2)$$

As a preventive measure against overfitting of the models to the training data, we implemented the "early stopping" technique. This technique, supported by the literature (HAYKIN, 2001; PRECHELT, 1998), allows for the interruption of training when there are no significant improvements in the performance of the models. Additionally, this decision is justified as a means of reducing the computational complexity of the models. After various tests on the training subset, the criteria for early stopping were established with a learning rate of α = 1 and a maximum number of iterations for the models set at 500. These values proved to be effective and suitable, regardless of the number of LCF considered in each model.

3.5. Performance evaluation

For each of the applied ML approaches, RF, LR, and ANN, the best models were evaluated. The performance evaluation of the models considered metrics widely used in studies related to ML and geosciences. This involved the use of ROC (Receiver Operating Characteristic) curves and confusion matrices. The ROC curve correlates the true positive rate (sensitivity) with the false positive rate (1 - specificity) at different threshold settings, thus providing a statistical index of overall model performance through the area under the ROC curve (AUC-ROC) (BEGUERÍA, 2006; CHUNG; FABBRI, 2003). Furthermore, performance metrics such as accuracy, precision, sensitivity, specificity, and F1-Score were extracted from the confusion matrix, calculated according to Equations 3 – 7 (e.g. BUI et al., 2020; EIRAS et al., 2021; JIAO et al., 2019; SINGH et al., 2023; SOLANKI; GUPTA; JOSHI, 2022). At the end of the calculations, the best models were selected based on the obtained values of accuracy, AUC-ROC (which encompasses both sensitivity and specificity), and F1-Score (which encompasses both precision and sensitivity).

$$accuracy = (TP + TN) \div (TP + TN + FP + FN) \quad (3)$$

$$precision = TP \div (TP + FP) \quad (4)$$

$$sensitivity = TP \div (TP + FN) \quad (5)$$

$$specificity = TN \div (TN + FP) \quad (6)$$

$$F1 - Score = \frac{2 * \text{precision} * sensitivity}{\text{precision} + sensitivity} \quad (7)$$

Where:

- TP = True positives;
- TN = True negatives;
- FP = False positives;
- FN = False negatives.

For each of the three adopted ML techniques, considering all possible configurations of the ML algorithms and variations in the input data (Section 3.4), we selected the best model developed by each algorithm and calculated the landslide susceptibility index for the study area. Subsequently, the resulting susceptibility maps were reclassified into three distinct susceptibility zones using the natural breaks classification method (Jenks), which were qualified into categories of low, moderate, and high susceptibility. Finally, we evaluated the efficiency of the classifications in the susceptibility maps based on the density of landslide areas present in the high and low susceptibility categories. In this context, we utilized the significance values of the Efficiency Rate (ER), in Equation 8, and Table 3, proposed by Chung and Fabbri (2003) and adapted by Guzzetti et al. (2006) for complex regions with a high incidence of landslides.

$$\text{ER}_i = \frac{(S \cap C_i)}{C_i} \div \frac{S}{\Omega} \quad (8)$$

Where:

- ER_i = Efficiency rate of class i;
- Ω = Entire study area;
- S = Area occupied by all landslides across the entire area Ω;
- C_i = Area of class i.

Table 3. Significance of the efficiency rate at susceptibility levels

Classification Efficiency		Efficiency Rate (ER)	
		Chung and Fabbri (2003)	Guzzetti et al. (2006)
High Susceptibility	Very significant	$\text{ER}_i > 6$	$\text{ER}_i > 1.5$
	Significant	$3 < \text{ER}_i \leq 6$	-
	Not significant	$0.2 \leq \text{ER}_i \leq 3$	$0.5 \leq \text{ER}_i \leq 1.5$
Low Susceptibility	Not significant	$0.2 \leq \text{ER}_i \leq 3$	$0.5 \leq \text{ER}_i \leq 1.5$
	Significant	$0.1 \leq \text{ER}_i < 0.2$	-
	Very significant	$\text{ER}_i < 0.1$	$\text{ER}_i < 0.5$

4. Results

4.1. Landslide conditioning factors (LCF)

The importance of each LCF is illustrated in Figure 5, according to the total IG value. It was observed that the slope angle is the most significant factor (IG = 0.486), followed by geomorphology (IG = 0.235), TWI (IG = 0.138), lithology (IG = 0.077), slope aspect (IG = 0.067), TPI (IG = 0.052), distance from drainage (IG = 0.032), slope curvature (IG = 0.029), and finally, the distance from the roads (IG = 0.024).

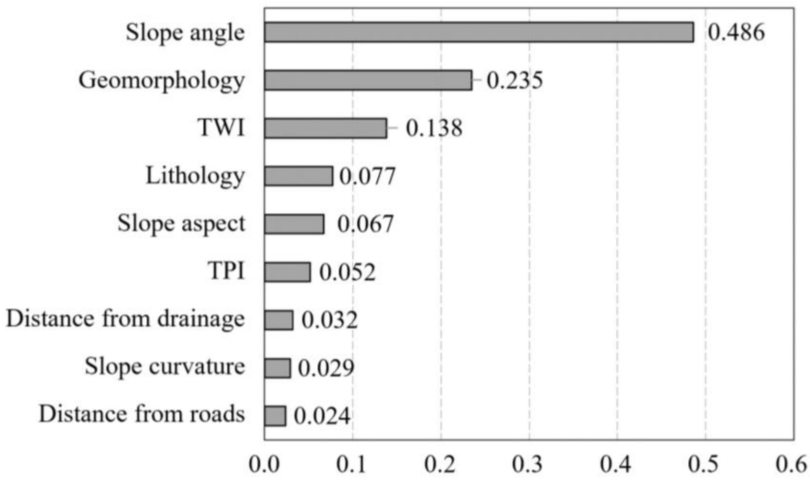

Figure 5. Importance of LCF according to IG values

4.2. Construction of the Landslide Susceptibility Models

According to Table 4, the RF models with the best performance are identified, considering the variation in the number of LCF used, ranging from four to nine. Additionally, Table 4 highlights the best RF model found (RF-6) based on accuracy, AUC-ROC, and the F1-Score values.

Table 4. Best developed RF models

Configurations	**Models**					
	RF-1	**RF-2**	**RF-3**	**RF-4**	**RF-5**	**RF-6**
Number of LCF	4	5	6	7	8	9
Number of decision trees	100	70	90	100	100	90
Number of LCF at nodes	4	5	6	5	6	3
AUC-ROC	0.922	0.923	0.940	0.941	0.942	0.947
Accuracy	0.850	0.851	0.867	0.873	0.872	0.878
Precision	0.846	0.844	0.861	0.865	0.862	0.858
Sensitivity	0.855	0.859	0.875	0.882	0.886	0.906
Specificity	0.845	0.842	0.859	0.863	0.858	0.850
F1-Score	0.850	0.852	0.868	0.874	0.874	0.881

Among the evaluated LR models, considering the variation from four to nine LCF, the ones that showed the best results were built using L2 regularization and C=0.01, as presented in Table 5. Furthermore, Table 5 highlights the best identified LR model (LR-4) based on the accuracy, AUC-ROC, and F1-Score values.

Table 5. Best developed LR models

Configurations	Models					
	LR-1	**LR-2**	**LR-3**	**LR-4**	**LR-5**	**LR-6**
Number of LCF	4	5	6	7	8	9
Regularization method	L2	L2	L2	L2	L2	L2
Regularization strength	0.1	0.1	0.1	0.1	0.1	0.1
AUC-ROC	0.929	0.931	0.935	0.936	0.935	0.935
Accuracy	0.874	0.874	0.875	0.885	0.884	0.882
Precision	0.852	0.851	0.852	0.862	0.860	0.859
Sensitivity	0.906	0.906	0.908	0.915	0.916	0.914
Specificity	0.843	0.842	0.843	0.854	0.851	0.850
F1-Score	0.878	0.878	0.879	0.888	0.887	0.886

According to Table 6, the ANN models that demonstrated the best performance were evaluated based on the variation in the number of LCF used, ranging from four to nine. Although model ANN-3 achieved the highest AUC-ROC score, its accuracy and F1-Score values were slightly lower than those of model ANN-1. This suggests that both models could be applied to landslide susceptibility modeling, as they present good statistical metrics. However, we opted to select ANN-3 for comparison with the other approaches used in the study, since AUC-ROC is one of the most widely adopted metrics for selecting the best ML models, as demonstrated by other authors (e.g. POURGHASEMI; RAHMATI, 2018; SARFRAZ et al., 2022).

Table 6. Best developed ANN models

Configurations	Models					
	ANN-1	**ANN-2**	**ANN-3**	**ANN-4**	**ANN-5**	**ANN-6**
Number of LCF	4	5	6	7	8	9
Number of neurons in the hidden layer	9	11	13	15	17	19
Activation function	ReLu	ReLu	ReLu	ReLu	ReLu	ReLu
Optimizer	Adam	Adam	Adam	Adam	Adam	Adam
Learning rate α	1	1	1	1	1	1
Limit of iterations	500	500	500	500	500	500
AUC-ROC	0.931	0.928	0.934	0.932	0.931	0.930
Accuracy	0.865	0.855	0.864	0.862	0.862	0.863
Precision	0.851	0.841	0.853	0.850	0.846	0.850
Sensitivity	0.886	0.876	0.881	0.879	0.885	0.881
Specificity	0.845	0.834	0.848	0.845	0.840	0.845
F1-Score	0.868	0.858	0.867	0.864	0.865	0.866

In order to compare the results, Figures 6, 7, and 8 present the susceptibility maps generated by the most effective model identified in each applied ML approach (RF-6, LR-4 and ANN-3).

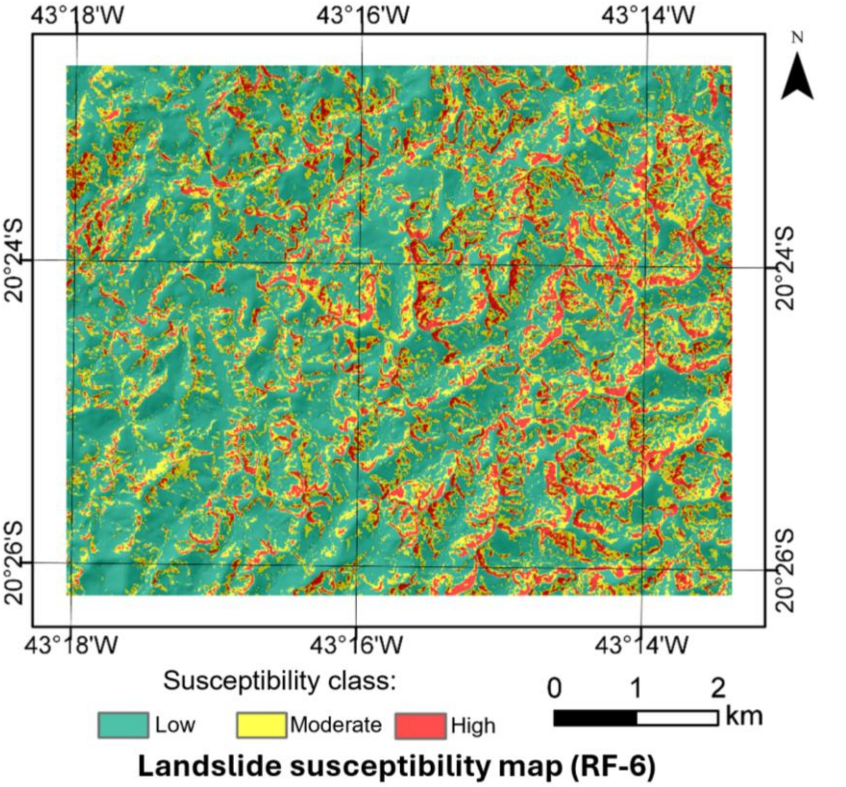

Figure 6. Landslide susceptibility map of the RF-6 model

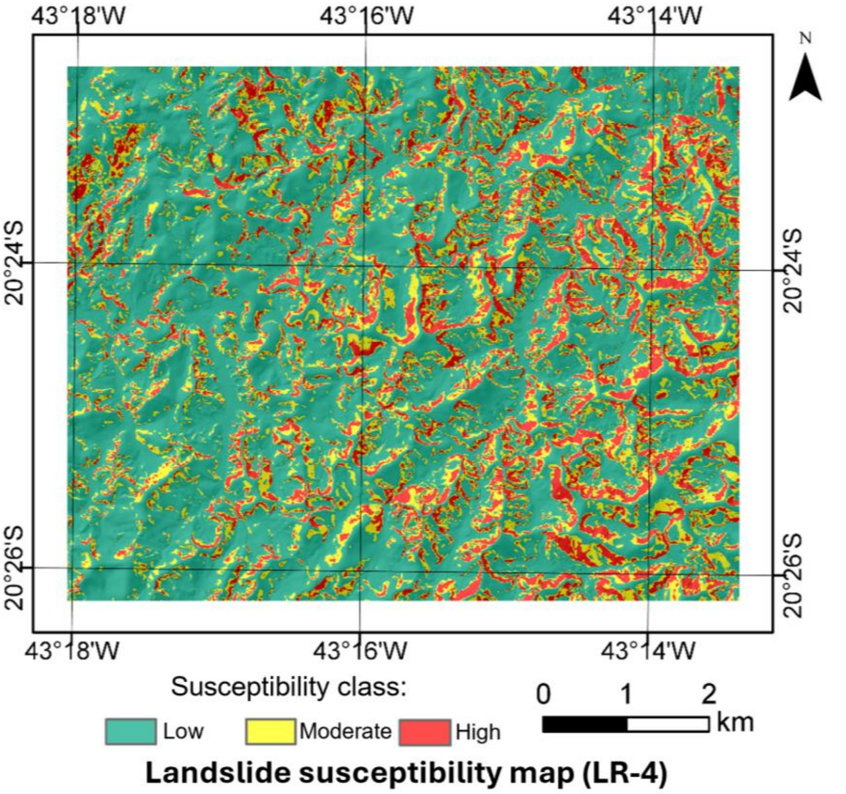

Figure 7. Landslide susceptibility map of the LR-4 model

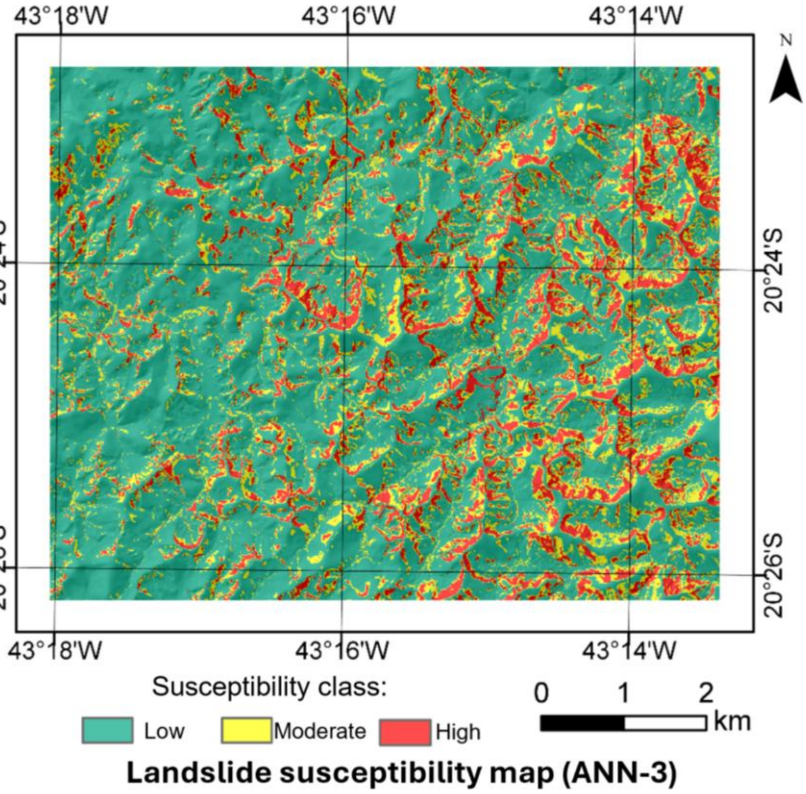

Figure 8. Landslide susceptibility map of the ANN-3 model

Regardless of the ML method employed, all susceptibility models exhibited high AUC-ROC values (RF-6 = 0.947, LR-4 = 0.936 and ANN-3 = 0.934), as shown in Figure 9.

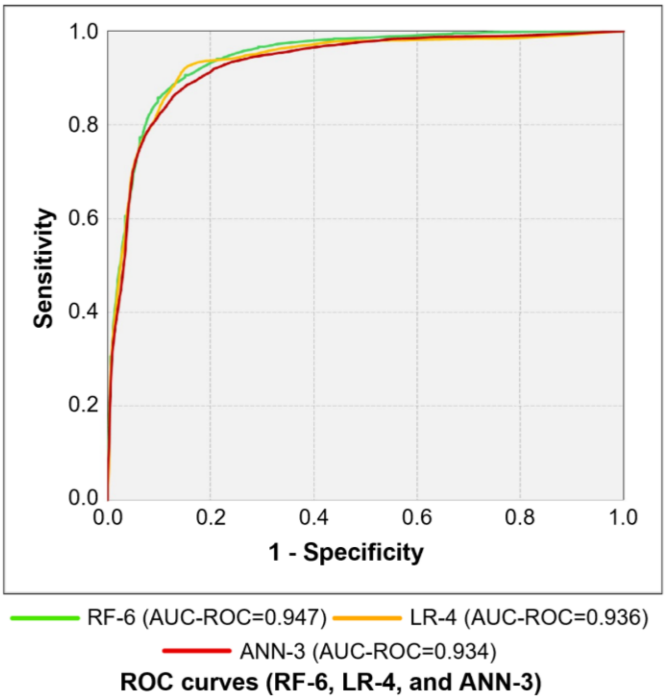

Figure 9. ROC Curves of the RF-6, LR-4 and ANN-3 models

The percentage of area assigned to each susceptibility class (low, moderate and high) and the efficiency rates calculated for the low (ER_i^{LS}) and high (ER_i^{HS}) susceptibility classes of each model are detailed in Table 7.

Table 7. Area (%) for each mapped landslide susceptibility class

Model	**Susceptibility class**			**Classification efficiency rate (ER_i)**	
	Low	**Moderate**	**High**	**Low susceptibility (ER_i^{LS})**	**High susceptibility (ER_i^{HS})**
RF-6	65.606%	19.526%	14.868%	0.030	6.808
LR-4	65.099%	19.497%	15.404%	0.050	5.695
ANN-3	69.325%	17.321%	13.354%	0.060	6.495

5. Discussions

The success of landslide susceptibility modeling directly depends on selecting the most appropriate statistical technique (FELICÍSIMO et al., 2013). Although several studies have compared different ML approaches, there is still no definitive consensus on which technique is the most effective. The selection of the most suitable approach depends on understanding the investigated process, as well as the availability and quality of the data. Therefore, it is crucial to conduct comparisons among different methodological techniques to determine the most appropriate for LSM in various contexts. The analyses conducted in our study, comparing the techniques of RF, LR and ANN for susceptibility mapping, contribute to this understanding, complementing previous research that investigated different ML approaches, such as the studies conducted by Akgun (2012), Chen et al. (2023), Liu et al. (2022), and Pham et al. (2016).

Pham et al. (2021) indicate the evaluation on the importance of LCF to enhance the generalization capacity of LSM models. In our research, by using the IG index for this purpose, we found that slope angle was the most significant factor for modeling susceptibility in the investigated region. Although this finding is aligned with other studies conducted in mountainous regions, such as those by Kumar et al. (2023), Youssef and Pourghasemi (2021), which highlighted the importance of slope angle in the predisposition to landslides, it is also important to consider that slope angle is not always the primary LCF. As emphasized by Micheletti et al. (2014), LCF are influenced by the intrinsic characteristics of the terrain and the local nature of landslides. Thus, the relevance of a specific factor may vary depending on the study area.

Although the removal of irrelevant LCF is an important step in susceptibility modeling, as indicated by Merghadi et al. (2020), our research did not identify significant variations in the results obtained due to this process. A slight variation in AUC-ROC was observed among the best-performing models, with the number of LCF considered alternating for each adopted ML technique: 2.5% for the RF technique, 0.7% for LR, and 0.6% for ANN (Table 8). This suggests that any of the best-performing models for each adopted ML technique would yield satisfactory results. However, for comparison purposes, we chose to use the models that achieved the highest AUC-ROC values, which were the RF-6 (AUC-ROC=0.947), LR-4 (AUC-ROC=0.936), and ANN-3 (AUC-ROC=0.934), constructed with the nine, seven, and six most important LCF, respectively. Our results indicated the effectiveness of all three models, with AUC-ROC values close to those found in the ML models evaluated by Youssef and Pourghasemi (2021), which ranged from 0.890 for the quadratic discriminant analysis technique to 0.951 for the RF, and higher than those evaluated by Pourghasemi and Rahmati (2018), which ranged from 0.624 for the generalized linear model technique to 0.837 for the RF.

Table 8. Variation of AUC-ROC observed in the best models of each adopted ML technique

Machine learning technique	**Model with the highest AUC-ROC value**	**Model with the lowest AUC-ROC value**	**Variation of AUC-ROC**
RF	0.947	0.922	2.5%
LR	0.936	0.929	0.7%
ANN	0.934	0.928	0.6%

The other statistical metrics analyzed for the models RF-6 (accuracy = 0.878, precision = 0.858, sensitivity = 0.906, specificity = 0.906, and F1 Score = 0.881), LR-4 (accuracy = 0.885, precision = 0.862, sensitivity = 0.915, specificity = 0.854, and F1 Score = 0.888), and ANN-3 (accuracy = 0.864, precision = 0.853, sensitivity = 0.881, specificity = 0.848, and F1 Score = 0.867) demonstrate that all the ML approaches utilized were effective in adequately and sensitively identifying areas susceptible to landslides, as well as in properly distinguishing non-susceptible areas. The values obtained for the analyzed metrics are comparable to those in previous studies that also demonstrated strong performances in the ML models evaluated (SHAHZAD; DING; ABBAS, 2022; WANG et al., 2021; ZHANG et al., 2022).

Additionally, we considered the ER for evaluating the models. For the classification of low susceptibility, the TE results for the best model of each ML technique (RF-6 = 0.03, LR-4 = 0.05 and ANN-3 = 0.06) demonstrated very significant efficiency, remaining within the limits defined by Chung and Fabbri (2003), and Guzzetti et al. (2006). Furthermore, the results demonstrated that the RF-6 model had the lowest number of areas with landslide occurrences in the low susceptibility range. Regarding the classification of high susceptibility, the ER results (RF-6 = 6.808, LR-4 = 5.695 and ANN-3 = 6.495) showed that the RF-6 and ANN-3 models achieved a high significant efficiency, while the LR-4 model achieved significant efficiency, according to the criteria established by Chung and Fabbri (2003). However, when considering the limits adapted by Guzzetti (2006) for the complex areas with a significant history of landslides, as is the case in the studied region, all three models demonstrated a very significant efficiency. Notably, for the classification of high susceptibility, the RF-6 model exhibited the highest ER value, indicating that the area delineated as high susceptibility by this model encompassed a larger extent of landslides compared to the ANN-3 and LR-4 models.

Considering all the evaluation metrics adopted, the three ML methodologies used to model landslide susceptibility in the study area demonstrated a remarkable compatibility of efficiency, making it difficult to determine which technique was superior. From a practical standpoint, any of the three LSM models produced would be capable of fulfilling its primary objective: predicting areas prone to future landslides and providing support in decision-making to prevent and mitigate these events. However, since the RF-6 model presented the best AUC-ROC and ER metrics for high and low susceptibility classes, we opted to select it to represent the landslide susceptibility of the study area.

6. Conclusion

The mapping of landslide susceptibility plays a crucial role in natural risk management. With the increasing incidence of landslides in various regions worldwide, particularly in the mountainous areas of Brazil, it becomes increasingly imperative to develop effective approaches to identify areas susceptible to these events. In this context, machine learning techniques emerge as promising tools capable of providing valuable insights for the prediction and mitigation of landslides. Thus, this research arrived at the following conclusions:

(1) The information gain index satisfactorily indicated the influence order of the conditioning factors in the modeling of landslide susceptibility, with slope being the most important factor, followed by geomorphology, TWI, lithology, slope orientation, TPI, distance from the drainage network, slope curvature, and distance from the roads;

(2) The best models produced by each statistical technique varied the number of conditioning factors considered, highlighting a close relationship between the machine learning algorithm and the peculiarities of the study area;

(3) The Random Forest, Logistic Regression, and Artificial Neural Networks approaches demonstrated good performances for the spatial prediction of landslides in the studied region. Although the results show statistical compatibility among the three approaches, the Random Forest model RF-6, which employed all available conditioning factors in the training, exhibited a high AUC-ROC (0.947) and very significant Efficiency Rate for the high and low susceptibility classes (ER_i^{HS} = 0.03 *e* ER_i^{LS} = 6.808). This model also demonstrated an accuracy of 87.8%, precision of 85.8%, sensitivity of 90.6%, specificity of 90.6%, and F1-Score of 88.1%, thus reinforcing its ability to pertinently predict areas susceptible to landslides;

(4) Machine learning approaches for mapping landslide susceptibility have demonstrated high predictive capacity, establishing themselves as a reliable and robust alternative for cartographic production, assisting engineers and decision-makers in the prevention and mitigation of landslides, especially in hard-to-reach areas such as mountainous regions;

(5) The development and improvement of statistical methodologies for mapping landslide susceptibility, particularly focusing on machine learning techniques, are still on the rise in the international context, especially in Brazil. In this scenario, these studies play a crucial role by providing valuable discussions and significantly contributing to the advancement of science

Authors' Contributions: Conceptualization, M.O.X. and C.F.B.; methodology, M.O.X.; validation, M.O.X.; formal analysis, M.O.X.; investigation, M.O.X.; data curation, M.O.X.; writing—original draft preparation, M.O.X. and C.F.B.; writing—review and editing, M.O.X. and C.F.B.; visualization, M.O.X.; supervision, C.F.B.; project administration, C.F.B. All authors have read and agreed to the published version of the manuscript.

Funding: This research did not receive any external funding.

Acknowledgments: The authors would like to express their sincere gratitude to the European Space Agency for providing free Sentinel-2 data and the Federal University of Ouro Preto (UFOP) and the Coordination for the Improvement of Higher Education Personnel (CAPES) of the Federal Government of Brazil for their support.

Conflict of Interest: The authors declare no conflicts of interest.

References

1. ABDELRAHMAN, M.M. **Instance-based Label Smoothing for Better Classifier Calibration.** Dissertação (Mestrado em Ciência da Computação) – Institute of Computer Science, University of Tartu, Tartu. 2020. 68p.
2. ABU EL-MAGD, S.A., ALI, S.A., PHAM, Q.B. Spatial modeling and susceptibility zonation of landslides using random forest, naïve bayes and K-nearest neighbor in a complicated terrain. **Earth Science Informatics**, V. 14, p. 1227–1243, 2021. DOI: 10.1007/s12145-021-00653-y
3. AGATONOVIC-KUSTRIN, S., BERESFORD, R. Basic concepts of artificial neural network (ANN) modeling and its application in pharmaceutical research. **Journal of Pharmaceutical and Biomedical Analysis**, V. 22, p. 717–727, 2000. DOI: 10.1016/S0731-7085(99)00272-1
4. AHRENDT, A., ZUQUETTE, L.V. Triggering factors of landslides in Campos do Jordão city, Brazil. **Bulletin of Engineering Geology and the Environment**, V. 62, p. 231–244, 2003. DOI: 10.1007/s10064-003-0191-8
5. AKGUN, A. A comparison of landslide susceptibility maps produced by logistic regression, multi-criteria decision, and likelihood ratio methods: A case study at İzmir, Turkey. **Landslides**, V. 9, 93–106, 2012. DOI: 10.1007/s10346-011-0283-7
6. ALALOUL, W.S., QURESHI, A.H. Data Processing Using Artificial Neural Networks. In: HARKUT, D.G. (Ed.). **Dynamic Data Assimilation - Beating the Uncertainties**. 1ª Ed. Londres: IntechOpen. 2020. DOI: 10.5772/intechopen.91935
7. ALEOTTI, P., CHOWDHURY, R. Landslide hazard assessment: summary review and new perspectives. **Bulletin of Engineering Geology and the Environment**, V. 58, p. 21–44, 1999. DOI: 10.1007/s100640050066
8. ANBAZHAGAN, S., SAJINKUMAR, K.S. Geoinformatics in Terrain Analysis and Landslide Susceptibility Mapping in Part of Western Ghats, India. In: ANBAZHAGAN, S., SUBRAMANIAN, S.K., YANG, X. (Eds.). **Geoinformatics in Applied Geomorphology**. 1ªEd. Boca Raton: CRC Press, 2011. p. 291–315.
9. ARMAŞ, I., VARTOLOMEI, F., STROIA, F., BRAŞOVEANU, L. Landslide susceptibility deterministic approach using geographic information systems: Application to Breaza town, Romania. **Natural Hazards**, V. 70, p. 995–1017, 2014. DOI: 10.1007/s11069-013-0857-x
10. BACHRI, S., SUMARMI, YUDHA IRAWAN, L., UTAYA, S., DWITRI NURDIANSYAH, F., ERFIKA NURJANAH, A., WAHYU NING TYAS, L., AMRI ADILLAH, A., SETIA PURNAMA, D. Landslide Susceptibility Mapping (LSM) in Kelud Volcano Using Spatial Multi-Criteria Evaluation. **IOP Conference Series: Earth and Environmental Science**. V. 273, 26p., 2019. DOI: 10.1088/1755-1315/273/1/012014
11. BARELLA, C.F., SOBREIRA, F.G., ZÊZERE, J.L. A comparative analysis of statistical landslide susceptibility mapping in the southeast region of Minas Gerais state, Brazil. **Bulletin of Engineering Geology and the Environment**. V. 78, p. 3205–3221, 2019. DOI: 10.1007/s10064-018-1341-3

12. BATISTA, P. **Avaliação geotécnica de misturas de um solo laterítico com cimento e bentonita para uso em cortinas verticais**. Dissertação (Mestrado em Geotecnia) – Programa de Pós-Graduação em Geotecnia, Universidade Federal de Ouro Preto, Ouro Preto. 2006. 100p.
13. BEGUERÍA, S. Validation and evaluation of predictive models in hazard assessment and risk management. **Natural Hazards**. V. 37, p. 315–329, 2006. DOI: 10.1007/s11069-005-5182-6
14. BISWAS, B., RAHAMAN, A., BARMAN, J. Comparative Assessment of FR and AHP Models for Landslide Susceptibility Mapping for Sikkim, India and Preparation of Suitable Mitigation Techniques. **Journal of the Geological Society of India**. V. 99, p. 791–801, 2023. DOI: 10.1007/s12594-023-2386-x
15. BISWAS, B., RANJAN, R. Landslide susceptibility mapping using integrated approach of multi-criteria and geospatial techniques at Nilgiris district of India. **Arabian Journal of Geosciences**. V. 14, 17p., 2021. DOI: 10.1007/s12517-021-07341-7
16. BLAIS-STEVENS, A., BEHNIA, P. Debris flow susceptibility mapping using a qualitative heuristic method and Flow-R along the Yukon Alaska Highway Corridor, Canada. **Natural Hazards and Earth System Sciences**. V. 16, p. 449–462, 2016. DOI: 10.5194/nhess-16-449-2016
17. BORGA, M., DALLA FONTANA, G., DA ROS, D., MARCHI, L. Shallow landslide hazard assessment using a physically based model and digital elevation data. **Environmental Geology**. V. 35, p. 81–88, 1998. DOI: 10.1007/s002540050295
18. BUI, D.T., TSANGARATOS, P., NGUYEN, V.T., LIEM, N. VAN, TRINH, P.T. Comparing the prediction performance of a Deep Learning Neural Network model with conventional machine learning models in landslide susceptibility assessment. **Catena**. V. 188, 14p., 2020. DOI: 10.1016/j.catena.2019.104426
19. CALDERÓN-GUEVARA, W., SÁNCHEZ-SILVA, M., NITESCU, B., VILLARRAGA, D.F. Comparative review of data-driven landslide susceptibility models: case study in the Eastern Andes mountain range of Colombia. **Natural Hazards**. V. 113, p. 1105–1132, 2022. DOI: 10.1007/s11069-022-05339-2
20. CARVALHO, T.R.R. DE, SOBREIRA, F.G., BARELLA, C.F., PEDROSA, M.A.F. Aptidão urbana na bacia hidrográfica do Rio Maracujá, município de Ouro Preto, MG. In: 14º Congresso Brasileiro de Geologia de Engenharia e Ambiental, 2013, Rio de Janeiro. **Anais...** Rio de Janeiro: ABGE. 2013.
21. CEMADEN, 2024. **Mapa Interativo da Rede Observacional para Monitoramento de Risco de Desastres Naturais**. Disponível em <http://www.cemaden.gov.br/mapainterativo>. Acesso em: 26-03-24.
22. CHACÓN, J., IRIGARAY, C., FERNÁNDEZ, T., EL HAMDOUNI, R. Engineering geology maps: Landslides and geographical information systems. **Bulletin of Engineering Geology and the Environment**. V. 65. p. 341-411, 2006. DOI: 10.1007/s10064-006-0064-z
23. CHEN, C., SHEN, Z., WENG, Y., YOU, S., LIN, J., LI, S., WANG, K. Modeling Landslide Susceptibility in Forest-Covered Areas in Lin'an, China, Using Logistical Regression, a Decision Tree, and Random Forests. **Remote Sensing**. V. 15, 19p., 2023. DOI: 10.3390/rs15184378
24. CHEN, F., YU, B., LI, B. A practical trial of landslide detection from single-temporal Landsat8 images using contour-based proposals and random forest: a case study of national Nepal. **Landslides**. V. 15, p. 453–464, 2018. DOI: 10.1007/s10346-017-0884-x
25. CHEN, T., NIU, R., JIA, X. A comparison of information value and logistic regression models in landslide susceptibility mapping by using GIS. **Environmental Earth Sciences**. V. 75, n. 867, 16p., 2016. DOI: 10.1007/s12665-016-5317-y
26. CHEN, W., POURGHASEMI, H.R., NAGHIBI, S.A. Prioritization of landslide conditioning factors and its spatial modeling in Shangnan County, China using GIS-based data mining algorithms. **Bulletin of Engineering Geology and the Environment**. V. 77, p. 611–629, 2018. DOI: 10.1007/s10064-017-1004-9
27. CHOWDHURY, M.S. A review on landslide susceptibility mapping research in Bangladesh. **Heliyon**. V. 9, 22p., 2023. DOI: 10.1016/j.heliyon.2023.e17972

28. CHUNG, C.-J.F., FABBRI, A.G. Validation of Spatial Prediction Models for Landslide Hazard Mapping, **Natural Hazards**. V. 30, p. 451-472, 2003. DOI: 10.1023/B:NHAZ.0000007172.62651.2b
29. COCO, L., MACRINI, D., PIACENTINI, T., BUCCOLINI, M. Landslide susceptibility mapping by comparing gis-based bivariate methods: A focus on the geomorphological implication of the statistical results. **Remote Sensing**. V. 13, 29p. 2021. DOI: 10.3390/rs13214280
30. CONFORTI, M., PASCALE, S., ROBUSTELLI, G., SDAO, F. Evaluation of prediction capability of the artificial neural networks for mapping landslide susceptibility in the Turbolo River catchment (northern Calabria, Italy). **Catena**. V. 113, p. 236–250, 2014. DOI: 10.1016/j.catena.2013.08.006
31. COROMINAS, J., VAN WESTEN, C., FRATTINI, P., CASCINI, L., MALET, J.P., FOTOPOULOU, S., CATANI, F., VAN DEN EECKHAUT, M., MAVROULI, O., AGLIARDI, F., PITILAKIS, K., WINTER, M.G., PASTOR, M., FERLISI, S., TOFANI, V., HERVÁS, J., SMITH, J.T. Recommendations for the quantitative analysis of landslide risk. **Bulletin of Engineering Geology and the Environment**. V. 73, p. 209–263, 2014. DOI: 10.1007/s10064-013-0538-8
32. COX, D.R. The Regression Analysis of Binary Sequences. **Journal of the Royal Statistical Society: Series B (Methodological)**. V. 20, p. 215–232, 1958. DOI: 10.1111/j.2517-6161.1958.tb00292.x
33. CRUZ, U.R.X.DA, OLIVEIRA, L.P.DE. Comparativo entre os métodos de classificação MaxVer e Random Forest utilizando imagem Sentinel-2B. **Cadernos do Leste**. V. 21, p. 1–19, 2021. DOI: 10.29327/248949.21.21-2
34. DAHAL, R.K., HASEGAWA, S., NONOMURA, A., YAMANAKA, M., MASUDA, T., NISHINO, K. GIS-based weights-of-evidence modelling of rainfall-induced landslides in small catchments for landslide susceptibility mapping. **Environmental Geology**. V. 54, p. 311–324, 2008. DOI: 10.1007/s00254-007-0818-3
35. DAO, D. VAN, JAAFARI, A., BAYAT, M., MAFI-GHOLAMI, D., QI, C., MOAYEDI, H., PHONG, T. VAN, LY, H.B., LE, T.T., TRINH, P.T., LUU, C., QUOC, N.K., THANH, B.N., PHAM, B.T. A spatially explicit deep learning neural network model for the prediction of landslide susceptibility. **Catena**. V. 188, 13p., 2020. DOI: 10.1016/j.catena.2019.104451
36. DEMSAR, J., CURK, T., ERJAVE, A., GORUP, C., HOCEVAR, T., MILUTINOVIC, M., MOZINA, M., POLAJNAR, M., TOPLAK, M., STARIC, A., STAJDOHAR, M., UMEK, L., ZAGAR, L., ZBONTAR, J., ZITNIK, M., ZUPAN, B. Orange: Data Mining Toolbox in Python. **Journal of Machine Learning Research**. V. 14, p. 2349–2353, 2013.
37. DIKAU, R. Derivatives from detailed geoscientific maps using computer methods. **Zeitschrift für Geomorphologie**. V. 2, n. 80, p. 45–55, 1990.
38. DO PINHO, T.M., AUGUSTO FILHO, O. Landslide susceptibility mapping using the infinite slope, SHALSTAB, SINMAP, and TRIGRS models in Serra do Mar, Brazil. **Journal of Mountain Science**. V. 19, p. 1018–1036, 2022. DOI: 10.1007/s11629-021-7057-z
39. DOMÍNGUEZ-CUESTA, M.J., JIMÉNEZ-SÁNCHEZ, M., COLUBI, A., GONZÁLEZ-RODRÍGUEZ, G. Modelling shallow landslide susceptibility: A new approach in logistic regression by using favourability assessment. **International Journal of Earth Sciences**. V. 99, p. 661–674, 2010. DOI: 10.1007/s00531-008-0414-0
40. EFIONG, J., ENI, D.I., OBIEFUNA, J.N., ETU, S.J. Geospatial modelling of landslide susceptibility in Cross River State of Nigeria. **Scientific African**. V. 14, 14p., 2021. DOI: 10.1016/j.sciaf.2021.e01032
41. EIRAS, C.G.S., SOUZA, J.R.G. DE, FREITAS, R.D.A. DE, BARELLA, C.F., PEREIRA, T.M. Discriminant analysis as an efficient method for landslide susceptibility assessment in cities with the scarcity of predisposition data. **Natural Hazards**. V. 107, p. 1427–1442, 2021. DOI: 10.1007/s11069-021-04638-4
42. ELMOULAT, M., BRAHIM, L.A., ELMAHSANI, A., ABDELOUAFI, A., MASTERE, M. Mass movements susceptibility mapping by using heuristic approach. Case study: province of Tétouan (North of Morocco). **Geoenvironmental Disasters**. V. 8, n. 20, 19p., 2021. DOI: 10.1186/s40677-021-00192-0
43. ENDO, I., GALBIATTI, H.F., DELGADO, C.E.R., OLIVEIRA, M.M.F. DE, ZAPPAROLI, A. DE C., MOURA, L.G.B. DE, PERES, G.G., OLIVEIRA, A.H. DE, ZAVAGLIA, G., DANDERFER, F.A., GOMES, C.J.S., CARNEIRO, M.A., NALINI JR.,

H.A., CASTRO, P. DE T.A., SUITA, M.T. DE F., TAZAVA, E., LANA, C. DE C., MARTINS-NETO, M.A., MARTINS, M. DE S., FERREIRA, F.F.A., FRANCO, A.P., ALMEIDA, L.G., ROSSI, D.Q., ANGELI, G., MADEIRA, T.J.A., PIASSA, L.R.A., MARIANO, D.F., CARLOS, D.U. **Mapa Geológico do Quadrilátero Ferrífero, Minas Gerais, Brasil**. Ouro Preto: Departamento de Geologia, Escola de Minas - UFOP - Centro de Estudos Avançados do Quadrilátero Ferrífero, 2019.

44. ESLAMINEZHAD, S.A., EFTEKHARI, M., AKBARI, M. GIS-Based Flood Risk Zoning Based On Data-Driven Models. **Journal of Hydraulic Structures**. V. 6, p. 75–98, 2020. DOI: 10.22055/jhs.2021.36629.1163
45. FELICÍSIMO, Á.M., CUARTERO, A., REMONDO, J., QUIRÓS, E. Mapping landslide susceptibility with logistic regression, multiple adaptive regression splines, classification and regression trees, and maximum entropy methods: A comparative study. **Landslides**. V. 10, p. 175–189, 2013. DOI: 10.1007/s10346-012-0320-1
46. FELL, R., COROMINAS, J., BONNARD, C., CASCINI, L., LEROI, E., SAVAGE, W.Z. Guidelines for landslide susceptibility, hazard and risk zoning for land use planning. **Engineering Geology**. 102, 85–98, 2008. DOI: 10.1016/j.enggeo.2008.03.022
47. FERNANDES, N.F., GUIMARÃES, R.F., GOMES, R.A.T., VIEIRA, B.C., MONTGOMERY, D.R., GREENBERG, H. Condicionantes Geomorfológicos dos Deslizamentos nas Encostas: Avaliação de Metodologias e Aplicação de Modelo de Previsão de Áreas Susceptíveis. **Revista Brasileira de Geomorfologia**. V. 2, p. 51–71, 2001. DOI: 10.20502/rbg.v2i1.8
48. GALLI, M., ARDIZZONE, F., CARDINALI, M., GUZZETTI, F., REICHENBACH, P. Comparing landslide inventory maps. **Geomorphology**. V. 94, p. 268–289, 2008. DOI: 10.1016/j.geomorph.2006.09.023
49. GARCIA, R.A.C. Metodologias de avaliação da perigosidade e risco associado a movimentos de vertente: aplicação na bacia do rio Alenquer. Tese (Doutorado em Geografia). Universidade de Lisboa, Lisboa. 2012. 437p.
50. GARDNER, M.W., DORLING, S.R. Artificial neural networks (the multilayer perceptron) - a review of applications in the atmospheric sciences. **Atmospheric Environment**. V. 32, p. 2627–2636, 1998. DOI: 10.1016/S1352-2310(97)00447-0
51. GRABOWSKI, D., LASKOWICZ, I., MAŁKA, A., RUBINKIEWICZ, J. Geoenvironmental conditioning of landsliding in river valleys of lowland regions and its significance in landslide susceptibility assessment: A case study in the Lower Vistula Valley, Northern Poland. **Geomorphology**. V. 419, 24p., 2022. 10.1016/j.geomorph.2022.108490
52. GUILLARD, C., ZEZERE, J. Landslide susceptibility assessment and validation in the framework of municipal planning in Portugal: The case of loures municipality. **Environmental Management.** V. 50, p. 721–735, 2012. DOI: 10.1007/s00267-012-9921-7
53. GUZZETTI, F., CARDINALI, M., REICHENBACH, P., CARRARA, A. Comparing landslide maps: A case study in the upper Tiber River basin, central Italy. **Environmental Management**. V. 25, p. 247–263, 2000. DOI: 10.1007/s002679910020
54. GUZZETTI, F., CARRARA, A., CARDINALI, M., REICHENBACH, P. Landslide hazard evaluation: a review of current techniques and their application in a multi-scale study, Central Italy. **Geomorphology**. V. 31, p. 181–216, 1999. DOI: 10.1016/S0169-555X(99)00078-1
55. GUZZETTI, F., REICHENBACH, P., ARDIZZONE, F., CARDINALI, M., GALLI, M. Estimating the quality of landslide susceptibility models. **Geomorphology**. V. 81, p. 166–184, 2006. DOI: 10.1016/j.geomorph.2006.04.007
56. GUZZETTI, F., REICHENBACH, P., CARDINALI, M., GALLI, M., ARDIZZONE, F. Probabilistic landslide hazard assessment at the basin scale. **Geomorphology**. V. 72, p. 272–299, 2005. DOI: 10.1016/j.geomorph.2005.06.002
57. HASTIE, T., TIBSHIRANI, R., FRIEDMAN, J. **The Elements of Statistical Learning: Data Mining, Inference, and Prediction**. 2ªEd. Nova York: Springer, 2009. 758p. DOI: 10.1007/978-0-387-84858-7
58. HAYKIN, S. **Redes neurais: princípios e prática [translation]**. Trans. Paulo Martins Engel. 2ªEd. Porto Alegre: Bookman, 2001. 898p.
59. HECHT-NIELSEN, R. Kolmogorov's Mapping Neural Network Existence Theorem. In: IEEE First Annual International Conference on Neural Networks, 1987, San Diego, California. **Proceedings…** Nova York: IEEE press. 1987. p. 11–14.

60. HENRIQUES, C., ZÊZERE, J.L., MARQUES, F., 2015. The role of the lithological setting on the landslide pattern and distribution. **Engineering Geology**. V. 189, p. 17–31. DOI: 10.1016/j.enggeo.2015.01.025
61. HIRYE, M.C.M., ALVES, D.S., FILARDO, A.S., MCPHEARSON, T., WAGNER, F. Assessing Landslide Drivers in Social–Ecological–Technological Systems: The Case of Metropolitan Region of São Paulo, Brazil. **Remote Sensing**. V. 15, 26p., 2023. DOI: 10.3390/rs15123048
62. HUANG, R., LI, W. Formation, distribution and risk control of landslides in China. **Journal of Rock Mechanics and Geotechnical Engineering**. V. 3, p. 97–116, 2011. DOI: 10.3724/sp.j.1235.2011.00097
63. JEBUR, M.N., PRADHAN, B., TEHRANY, M.S. Manifestation of LiDAR-derived parameters in the spatial prediction of landslides using novel ensemble evidential belief functions and support vector machine models in GIS. **IEEE Journal of Selected Topics in Applied Earth Observations and Remote Sensing**. V. 8, n. 2, p. 674–690, 2015. DOI: 10.1109/JSTARS.2014.2341276
64. JENNIFER, J.J. Feature elimination and comparison of machine learning algorithms in landslide susceptibility mapping. **Environmental Earth Sciences**. V. 81, n. 489, 23p., 2022. DOI: 10.1007/s12665-022-10620-5
65. JIAO, Y., ZHAO, D., DING, Y., LIU, Y., XU, Q., QIU, Y., LIU, C., LIU, Z., ZHA, Z., LI, R. Performance evaluation for four GIS-based models purposed to predict and map landslide susceptibility: A case study at a World Heritage site in Southwest China. **Catena**. V. 183, 15p., 2019. DOI: 10.1016/j.catena.2019.104221
66. JOVANČEVIC, S.D., NAGAI, O., SASSA, K., ARBANAS, Ž. TXT-tool 3.385-1.2 deterministic landslide susceptibility analyses using LS-rapid software. In: SASSA, K. TIWARI, B., LIU, K., MCSAVENEY, M., STROM, A., SETIAWAN, H. (Eds.). **Landslide Dynamics: ISDR-ICL Landslide Interactive Teaching Tools. Volume 2: Testing, Risk Management and Country Practices**. Springer International Publishing, 2018. p. 169–179. Doi: 10.1007/978-3-319-57777-7_7
67. KAVZOGLU, T., SAHIN, E.K., COLKESEN, I. Landslide susceptibility mapping using GIS-based multi-criteria decision analysis, support vector machines, and logistic regression. **Landslides**. V. 11, p. 425–439, 2014. DOI: 10.1007/s10346-013-0391-7
68. KAVZOGLU, T., TEKE, A. Ensemble Conditioning Factor Selection with Markov Chain Framework for Shallow Landslide Susceptibility Mapping in Lake Sapanca Basin and its Vicinity, Turkey. **Baltic Journal of Modern Computing**. V. 10, p. 224–240, 2022. DOI: 10.22364/bjmc.2022.10.2.09
69. KINGMA, D.P., BA, J.L. Adam: A Method for Stochastic Optimization. **ArXiv preprint**. 15p., 2014. DOI: 10.48550/arXiv.1412.6980
70. KOPPE, G., MEYER-LINDENBERG, A., DURSTEWITZ, D. Deep learning for small and big data in psychiatry. **Neuropsychopharmacology**. V. 46, p. 176–190, 2021. DOI: 10.1038/s41386-020-0767-z
71. KUMAR, C., WALTON, G., SANTI, P., LUZA, C. An Ensemble Approach of Feature Selection and Machine Learning Models for Regional Landslide Susceptibility Mapping in the Arid Mountainous Terrain of Southern Peru. **Remote Sensing**. V. 15, 34p., 2023. DOI: 10.3390/rs15051376
72. LEE, S. Application of logistic regression model and its validation for landslide susceptibility mapping using GIS and remote sensing data. **International Journal of Remote Sensing**. V. 26, p. 1477–1491, 2005. DOI: 10.1080/01431160412331331012
73. LEE, S. Application of likelihood ratio and logistic regression models to landslide susceptibility mapping using GIS. **Environmental Management**. V. 34, p. 223–232, 2004. DOI: 10.1007/s00267-003-0077-3
74. LEE, S., MIN, K. Statistical analysis of landslide susceptibility at Yongin, Korea. **Environmental Geology**. V. 40, p. 1095–1113, 2001. DOI: 10.1007/s002540100310
75. LEE, SUNMIN, LEE, M.J., LEE, SARO. Spatial prediction of urban landslide susceptibility based on topographic factors using boosted trees. **Environmental Earth Sciences**. V. 77, n. 656, 22p., 2018. DOI: 10.1007/s12665-018-7778-7

76. LI, X., CHONG, J., LU, Y., LI, Z. Application of information gain in the selection of factors for regional slope stability evaluation. **Bulletin of Engineering Geology and the Environment**. V. 81, 15p., 2022. DOI: 10.1007/s10064-022-02970-y
77. LIMA, P., STEGER, S., GLADE, T., MURILLO-GARCIA, F.G. Literature Review and Bibliometric Analysis on Data-Driven Assessment of Landslide Susceptibility. **Journal of Mountain Science.** V. 19, p. 1670-1698, 2022. DOI: 10.1007/s11629-021-7254-9
78. LIU, R., YANG, X., XU, C., WEI, L., ZENG, X. Comparative Study of Convolutional Neural Network and Conventional Machine Learning Methods for Landslide Susceptibility Mapping. **Remote Sensing**. V. 14, 31p., 2022. DOI: 10.3390/rs14020321
79. LOTT, B.A., MAGALHÃES, M.E.O.C., CUNHA, D.M., PANQUESTOR, E.K., DA SILVA, R.V. Chuvas na Bacia Hidrográfica do Rio Doce – MG/ES no primeiro trimestre de 2020, in: **Sociedade, Tecnologia e Meio Ambiente: avanços, retrocessos e novas perspectivas**. Editora Científica Digital, pp. 110–126. 2021. DOI: 10.37885/210906068
80. MASCANZONI, E., PEREGO, A., MARCHI, N., SCARABEL, L., PANOZZO, S., FERRERO, A., ACUTIS, M., SATTIN, M. Epidemiology and agronomic predictors of herbicide resistance in rice at a large scale. **Agronomy for Sustainable Development**. V. 38, n. 68, 10p., 2018. DOI: 10.1007/s13593-018-0548-9
81. MAURIZIO, L., MARIA, D. A multi temporal kernel density estimation approach for new triggered landslides forecasting and susceptibility assessment. **Disaster Advances**. V. 5, p. 100–108, 2012.
82. MCCULLOCH, W.S., PITTS, W. A logical calculus of the ideas immanent in nervous activity. **Bulletin of Mathematical Biophysics**. V. 5, p. 115–133, 1943. DOI: 10.1007/BF02478259
83. MERGHADI, A., YUNUS, A.P., DOU, J., WHITELEY, J., THAIPHAM, B., BUI, D.T., AVTAR, R., ABDERRAHMANE, B. Machine learning methods for landslide susceptibility studies: A comparative overview of algorithm performance. **Earth-Science Reviews**. V. 207, 47p., 2020. DOI: 10.1016/j.earscirev.2020.103225
84. MICHEL, G.P., KOBIYAMA, M., GOERL, R.F. Comparative analysis of SHALSTAB and SINMAP for landslide susceptibility mapping in the Cunha River basin, southern Brazil. **Journal of Soils and Sediments**. V. 14, p. 1266–1277, 2014. DOI: 10.1007/s11368-014-0886-4
85. MICHELETTI, N., FORESTI, L., ROBERT, S., LEUENBERGER, M., PEDRAZZINI, A., JABOYEDOFF, M., KANEVSKI, M. Machine Learning Feature Selection Methods for Landslide Susceptibility Mapping. **Mathematical Geosciences**. V. 46, p. 33–57, 2014. DOI: 10.1007/s11004-013-9511-0
86. MIRANDA, C.E.B., BOMBACINI, M.R. Aplicação da Regressão Logística Binária para Manutenção Preditiva em Máquinas de Ressonância Magnética. In: XIII Congresso Brasileiro de Engenharia de Produção, 2023. **Anais…** APREPRO, 2023. 12p.
87. MOORE, I.D., GRAYSON, R.B., LADSON, A.R. Digital terrain modelling: A review of hydrological, geomorphological, and biological applications. **Hydrological Processes**. V. 5, p. 3–30, 1991. DOI: 10.1002/hyp.3360050103
88. MOULOODI, S., RAHMANPANAH, H., GOHARI, S., BURVILL, C., TSE, K.M., DAVIES, H.M.S. What can artificial intelligence and machine learning tell us? A review of applications to equine biomechanical research. **Journal of the Mechanical Behavior of Biomedical Materials**. V. 123, 13p., 2021. DOI: 10.1016/j.jmbbm.2021.104728
89. MURILLO-GARCÍA, F.G., ALCÁNTARA-AYALA, I. Landslide susceptibility analysis and mapping using statistical multivariate techniques: Pahuatlán, Puebla, Mexico. In: WU, W. (Ed.). **Recent Advances in Modeling Landslides and Debris Flows.** Springer Series in Geomechanics and Geoengineering. Springer, Cham, 2015. p. 179–194, 2015. DOI: 10.1007/978-3-319-11053-0_16
90. NAEMITABAR, M., ZANGANEH ASADI, M. Landslide zonation and assessment of Farizi watershed in northeastern Iran using data mining techniques. **Natural Hazards**. V. 108, p. 2423-2453, 2021. DOI: 10.1007/s11069-021-04805-7
91. NAIR, V., HINTON, G.E. Rectified Linear Units Improve Restricted Boltzmann Machines, In: 27th International Conference on Machine Learning (ICML), 2010, Haifa, Israel. **Anais…** 2010, p. 807–814.

92. NASKATH, J., SIVAKAMASUNDARI, G., BEGUM, A.A.S. A Study on Different Deep Learning Algorithms Used in Deep Neural Nets: MLP SOM and DBN. **Wireless Personal Communications**. V. 128, p. 2913–2936, 2023. DOI: 10.1007/s11277-022-10079-4
93. NEFESLIOGLU, H.A., DUMAN, T.Y., DURMAZ, S. Landslide susceptibility mapping for a part of tectonic Kelkit Valley (Eastern Black Sea region of Turkey). **Geomorphology**. V. 94, p. 401–418, 2008. DOI: 10.1016/j.geomorph.2006.10.036
94. NG, A.Y. Feature selection, L 1 vs. L 2 regularization, and rotational invariance. In: 21th International Conference on Machine Learning, 2004, Banff, Alberta, Canada. **Proceedings…** Nova York: Association for Computing Machinery, 2004. 8p. DOI: 10.1145/1015330.1015435
95. NHU, V.H., HOANG, N.D., NGUYEN, H., NGO, P.T.T., THANH BUI, T., HOA, P.V., SAMUI, P., TIEN BUI, D. Effectiveness assessment of Keras based deep learning with different robust optimization algorithms for shallow landslide susceptibility mapping at tropical area. **Catena**. V. 188, 13p., 2020. DOI: 10.1016/j.catena.2020.104458
96. NOHANI, E., MOHARRAMI, M., SHARAFI, S., KHOSRAVI, K., PRADHAN, B., PHAM, B.T., LEE, S., MELESSE, A.M. Landslide susceptibility mapping using different GIS-Based bivariate models. **Water**. V. 11, 22p., 2019. DOI: 10.3390/w11071402
97. NOLA, I.T. DE S. Análise multicritério e aprendizado de máquina aplicados na predição do potencial espeleológico da região do Parque Nacional Serra do Gandarela, Quadrilátero Ferrífero/MG. Tese (Doutorado em Geotecnia). Programa de Pós-Graduação em Geotecnia, Universidade Federal de Ouro Preto, Ouro Preto. 2022. 138p.
98. OGILA, W.A.M. Analysis and assessment of slope instability along international mountainous road in North Africa. **Natural Hazards**. V. 106, p. 2479–2517, 2021. DOI: 10.1007/s11069-021-04552-9
99. OH, H.J., LEE, S. Landslide susceptibility mapping on Panaon Island, Philippines using a geographic information system. **Environmental Earth Sciences**. V. 62, p. 935–951, 2011. DOI: 10.1007/s12665-010-0579-2
100. OHLMACHER, G.C. Plan curvature and landslide probability in regions dominated by earth flows and earth slides. **Engineering Geology**. V. 91, p. 117–134, 2007. DOI: 10.1016/j.enggeo.2007.01.005
101. OLIVEIRA, G.G. DE, RUIZ, L.F.C., GUASSELLI, L.A., HAETINGER, C. Random forest and artificial neural networks in landslide susceptibility modeling: a case study of the Fão River Basin, Southern Brazil. **Natural Hazards**. V. 99, p. 1049–1073, 2019. DOI: 10.1007/s11069-019-03795-x
102. PANDEY, V.H.R., KAINTHOLA, A., SHARMA, V., SRIVASTAV, A., JAYAL, T., SINGH, T.N. Deep learning models for large-scale slope instability examination in Western Uttarakhand, India. **Environmental Earth Sciences**. V. 81, n. 487, 18p., 2022. DOI: 10.1007/s12665-022-10590-8
103. PARK, Y.S., LEK, S. Artificial Neural Networks: Multilayer Perceptron for Ecological Modeling. In: JØRGENSEN, S.E. **Developments in Environmental Modelling**. Elsevier B.V., 2016. p. 123–140. DOI: 10.1016/B978-0-444-63623-2.00007-4
104. PAUL, S.G., BISWAS, A.A., SAHA, A., ZULFIKER, M.S., RITU, N.A., ZAHAN, I., RAHMAN, M., ISLAM, M.A. A real-time application-based convolutional neural network approach for tomato leaf disease classification. **Array**. V. 19, 14p., 2023. DOI: 10.1016/j.array.2023.100313
105. PAWLUSZEK, K., BORKOWSKI, A. Impact of DEM-derived factors and analytical hierarchy process on landslide susceptibility mapping in the region of Rożnów Lake, Poland. **Natural Hazards**. V. 86, p. 919–952, 2017. DOI: 10.1007/s11069-016-2725-y
106. PHAM, B.T., BUI, D.T., DHOLAKIA, M.B., PRAKASH, I., PHAM, H.V., MEHMOOD, K., LE, H.Q. A novel ensemble classifier of rotation forest and Naïve Bayer for landslide susceptibility assessment at the Luc Yen district, Yen Bai Province (Viet Nam) using GIS. **Geomatics, Natural Hazards and Risk**. V. 8, p. 649–671, 2017. DOI: 10.1080/19475705.2016.1255667

107. PHAM, B.T., PRADHAN, B., TIEN BUI, D., PRAKASH, I., DHOLAKIA, M.B. A comparative study of different machine learning methods for landslide susceptibility assessment: A case study of Uttarakhand area (India). **Environmental Modelling and Software**. V. 84, p. 240–250, 2016. DOI: 10.1016/j.envsoft.2016.07.005

108. PHAM, B.T., SHIRZADI, A., SHAHABI, H., OMIDVAR, E., SINGH, S.K., SAHANA, M., ASL, D.T., AHMAD, B. BIN, QUOC, N.K., LEE, S. Landslide susceptibility assessment by novel hybrid machine learning algorithms. **Sustainability**. V. 11, 25p., 2019. DOI: 10.3390/su11164386

109. PHAM, B.T., VAN DAO, D., ACHARYA, T.D., VAN PHONG, T., COSTACHE, R., VAN LE, H., NGUYEN, H.B.T., PRAKASH, I. Performance assessment of artificial neural network using chi-square and backward elimination feature selection methods for landslide susceptibility analysis. **Environmental Earth Sciences**. V. 80, n. 686, 13p., 2021. DOI: 10.1007/s12665-021-09998-5

110. PIMIENTO, E. **Shallow Landslide Susceptibility Modelling and Validation**. Dissertação (Mestrado em Ciência da Informação Geográfica). Department of Physical Geography and Ecosystem Analysis Centre for Geographical Information Systems, Lund University, Lund, Sweden. 2010. 104p.

111. PINHEIRO, M.A.P., MAGALHÃES, J.R., SILVA, M.A. DA, 2023. **Carta geológica: SF.23-X-B-I-3-SE (em revisão)**. Programa Geologia, Mineração e Transformação Mineral: Ação Levantamentos Geológicos e Integração Geológica Regional. Serviço Geológico do Brasil – SGB, 2023. 1:25.000

112. POURGHASEMI, H.R., KERLE, N. Random forests and evidential belief function-based landslide susceptibility assessment in Western Mazandaran Province, Iran. **Environmental Earth Sciences**. V. 75, p. 1–17, 2016. DOI: 10.1007/s12665-015-4950-1

113. POURGHASEMI, H.R., PRADHAN, B., GOKCEOGLU, C., DEYLAMI MOEZZI, K. Landslide susceptibility mapping using a spatial multi criteria evaluation model at haraz watershed, Iran. In: PRADHAN, B., BUCHROITHNER, M. (Ed.). **Terrigenous Mass Movements: Detection, Modelling, Early Warning and Mitigation Using Geoinformation Technology**. Berlin: Springer, 2012. p. 23–49. DOI: 10.1007/978-3-642-25495-6_2

114. POURGHASEMI, H.R., RAHMATI, O. Prediction of the landslide susceptibility: Which algorithm, which precision? **Catena**. V. 162, p. 177–192, 2018. DOI: 10.1016/j.catena.2017.11.022

115. POURGHASEMI, H.R., TEIMOORI YANSARI, Z., PANAGOS, P., PRADHAN, B. Analysis and evaluation of landslide susceptibility: a review on articles published during 2005–2016 (periods of 2005–2012 and 2013–2016). **Arabian Journal of Geosciences**. V. 11, 12p., 2018. DOI: 10.1007/s12517-018-3531-5

116. PRADHAN, B., SEENI, M.I., KALANTAR, B. Performance evaluation and sensitivity analysis of expert-based, statistical, machine learning, and hybrid models for producing landslide susceptibility maps. In: PRADHAN, B. (Ed.). **Laser Scanning Applications in Landslide Assessment**. Berlin: Springer, 2017. p. 193–232. DOI: 10.1007/978-3-319-55342-9_11

117. PRECHELT, L. Early Stopping - But When? In: ORR, G.B., MÜLLER, K.-R. (Eds.). **Neural Networks: Tricks of the Trade**. Berlin, Heidelberg, New York, Barcelona, Hong Kong, London, Milan, Paris, Singapore, Tokyo: Springer, 1998. p. 55–69. DOI: 10.1007/978-3-642-35289-8_5

118. QGIS DEVELOPMENT TEAM. **QGIS Geographic Information System (versão 3.12.3)**. 2020. Disponível em: <http://qgis.osgeo.org>.

119. QUINLAN. Induction of Decision Trees. **Machine Learning**. V. 1, p. 81–106, 1986. DOI: 10.1007/BF00116251

120. RAHMATI, O., HAGHIZADEH, A., POURGHASEMI, H.R., NOORMOHAMADI, F. Gully erosion susceptibility mapping: the role of GIS-based bivariate statistical models and their comparison. **Natural Hazards**. V. 82, p. 1231–1258, 2016. DOI: 10.1007/s11069-016-2239-7

121. REICHENBACH, P., ROSSI, M., MALAMUD, B.D., MIHIR, M., GUZZETTI, F. A review of statistically-based landslide susceptibility models. **Earth-Science Reviews**. V. 180, p. 60–91, 2018. DOI: 10.1016/j.earscirev.2018.03.001

122. RUFF, M., CZURDA, K. Landslide susceptibility analysis with a heuristic approach in the Eastern Alps (Vorarlberg, Austria). **Geomorphology**. V. 94, p. 314–324, 2008. DOI: 10.1016/j.geomorph.2006.10.032

123. SAHIN, E.K., COLKESEN, I., ACMALI, S.S., AKGUN, A., AYDINOGLU, A.C. Developing comprehensive geocomputation tools for landslide susceptibility mapping: LSM tool pack. **Computers & Geosciences**. V. 144, 16p., 2020. DOI: 10.1016/j.cageo.2020.104592

124. SANTACANA, N., BAEZA, B., COROMINAS, J., DE PAZ, A., MARTURIÁ, J. A GIS-Based Multivariate Statistical Analysis for Shallow Landslide Susceptibility Mapping in La Pobla de Lillet Area (Eastern Pyrenees, Spain). **Natural Hazards**. V. 30, p. 281–295, 2003. DOI: 10.1023/B:NHAZ.0000007169.28860.80

125. SARFRAZ, Y., BASHARAT, M., RIAZ, M.T., AKRAM, M.S., XU, C., AHMED, K.S., SHAHZAD, A., AL-ANSARI, N., LINH, N.T.T. Application of statistical and machine learning techniques for landslide susceptibility mapping in the Himalayan road corridors. **Open Geosciences**. V. 14, p. 1606–1635, 2022. DOI: 10.1515/geo-2022-0424

126. SEPÚLVEDA, S.A., PETLEY, D.N. Regional trends and controlling factors of fatal landslides in Latin America and the Caribbean. **Natural Hazards and Earth System Sciences**. V. 15, p. 1821–1833, 2015. DOI: 10.5194/nhess-15-1821-2015

127. SHAHABI, H., AHMADI, R., ALIZADEH, M., HASHIM, M., AL-ANSARI, N., SHIRZADI, A., WOLF, I.D., ARIFFIN, E.H. Landslide Susceptibility Mapping in a Mountainous Area Using Machine Learning Algorithms. **Remote Sensing**. V. 15, 18p., 2023. DOI: 10.3390/rs15123112

128. SHAHZAD, N., DING, X., ABBAS, S. A Comparative Assessment of Machine Learning Models for Landslide Susceptibility Mapping in the Rugged Terrain of Northern Pakistan. **Applied Sciences**. V. 12, 23p., 2022. DOI: 10.3390/app12052280

129. SHIRANI, K., PASANDI, M., ARABAMERI, A. Landslide susceptibility assessment by Dempster–Shafer and Index of Entropy models, Sarkhoun basin, Southwestern Iran. **Natural Hazards**. V. 93, p. 1379–1418, 2018. DOI: 10.1007/s11069-018-3356-2

130. SIDUMO, B., SONONO, E., TAKAIDZA, I. An approach to multi-class imbalanced problem in ecology using machine learning. **Ecological Informatics**. V. 71, 8p., 2022. DOI: 10.1016/j.ecoinf.2022.101822

131. SINGH, A., ASHULI, A., NIRAJ, K.C., DHIMAN, N., DUBEY, C.S., SHUKLA, D.P. Evaluating causative factors for landslide susceptibility along the Imphal-Jiribam railway corridor in the North-Eastern part of India using a GIS-based statistical approach. **Environmental Science and Pollution Research**. 18p. 2023. DOI: 10.1007/s11356-023-28966-z

132. SOBREIRA, F.G., SOUZA, L.A. DE, BARELLA, C.F., PEDROSA, M.A.F., CARVALHO, T.R. DE, SILVA, N. DE L. Elaboração de Cartas Geotécnicas de Aptidão à Urbanização Frente aos Desastres Naturais no Município de Ouro Preto, MG: Carta de Aptidão à Urbanização da Bacia do Rio Maracujá Escala 1:25000. Ouro Preto: 2013. UFOP.

133. SOETERS, R., VAN WESTEN, C.J. Slope instability recognition, analysis and zonation. In: A.K. TURNER, R.L. SHUSTER (Eds.). **Landslides: Investigation and Mitigation**. Idaho: Transportation Research Board, National Research Council, 1996. p. 129–177.

134. SOLANKI, A., GUPTA, V., JOSHI, M. Application of machine learning algorithms in landslide susceptibility mapping, Kali Valley, Kumaun Himalaya, India. **Geocarto International**. V. 37, p. 16846–16871, 2022. DOI: 10.1080/10106049.2022.2120546

135. SOUZA, L.A. DE. Cartografia geoambiental e cartografia geotécnica progressiva em diferentes escalas: aplicação na bacia hidrográfica do Ribeirão do Carmo, município de Ouro Preto e Mariana, Minas Gerais. Tese (Doutorado em Geotecnia). Programa de Pós-Graduação em Geotecnia, Universidade Federal de Ouro Preto, Ouro Preto. 2015. 461p.

136. SOUZA, L.A. DE. **Diagnóstico do meio físico como contribuição ao ordenamento territorial do município de Mariana – MG**. Dissertação (Mestrado em Geotecnia). rograma de Pós-Graduação em Geotecnia, Universidade Federal de Ouro Preto, Ouro Preto. 2004. 182p.

137. SOUZA, L.A. DE., SOBREIRA F.G. Proposta de unidades geomorfológicas como suporte ao planejamento urbano e ordenamento territorial. **Revista Brasileira de Geomorfologia**. V. 18, n. 4, 703-717, 2017. DOI: https://doi.org/10.20502/rbg.v18i4.1235

138. SOUZA, M.A.A. DE, SOUZA, L.A. DE, COELHO, G.L.L.M., MELO, A.L. DE. Levantamento malacológico e mapeamento das áreas de risco para transmissão da esquistossomose mansoni no Município de Mariana, Minas Gerais, Brasil. **Revista de Ciências Médicas e Biológicas**. V. 5, p. 132–139, 2006.

139. STANLEY, T., KIRSCHBAUM, D.B. A heuristic approach to global landslide susceptibility mapping. **Natural Hazards**. V. 87, p. 145–164, 2017. DOI: 10.1007/s11069-017-2757-y

140. TANOLI, J.I., JEHANGIR, A., QASIM, M., REHMAN, M. UR, SHAH, S.T.H., ALI, M., JADOON ISHTIAQ AHMAD KHAN. Application of bivariate statistical techniques for landslide susceptibility mapping: A case study in Kaghan Valley, NW Pakistan. **Geological Journal**. V. 58, p. 4576–4595, 2023.

141. THANH, L.N., DE SMEDT, F. Application of an analytical hierarchical process approach for landslide susceptibility mapping in A Luoi district, Thua Thien Hue Province, Vietnam. **Environmental Earth Sciences**. V. 66, p. 1739–1752, 2012. DOI: 10.1007/s12665-011-1397-x

142. TIAGO DAMAS, M., BIANCA CARVALHO, V., NELSON FERREIRA, F., CHISATO, O., DAVID R., M. Application of the SHALSTAB model for the identification of areas susceptible to landslides: Brazilian case studies. **Revista de Geomorfologie**. V. 19, p. 136–144, 2017. DOI: 10.21094/rg.2017.015

143. TSAI, F., LAI, J.S., CHEN, W.W., LIN, T.H. Analysis of topographic and vegetative factors with data mining for landslide verification. **Ecological Engineering**. V. 61, p. 669–677, 2013. DOI: 10.1016/j.ecoleng.2013.07.070

144. TZOUVARAS, M. Statistical time-series analysis of interferometric coherence from sentinel-1 sensors for landslide detection and early warning. **Sensors**. V. 21, 19p., 2021. DOI: 10.3390/s21206799

145. UEHARA, T.D.T., PASSOS CORRÊA, S.P.L., QUEVEDO, R.P., KÖRTING, T.S., DUTRA, L.V., RENNÓ, C.D. Landslide scars detection using remote sensing and pattern recognition techniques: Comparison among artificial neural networks, gaussian maximum likelihood, random forest, and support vector machine classifiers. **Revista Brasileira de Cartografia**. V. 72, p. 665–680, 2020. DOI: 10.14393/rbcv72n4-54037

146. ULLAH, I., ASLAM, B., SHAH, S.H.I.A., TARIQ, A., QIN, S., MAJEED, M., HAVENITH, H.B. An Integrated Approach of Machine Learning, Remote Sensing, and GIS Data for the Landslide Susceptibility Mapping. **Land**. V. 11, 20p., 2022. DOI: 10.3390/land11081265

147. WALKER, S.H., DUNCAN, D.B. Estimation of the Probability of an Event as a Function of Several Independent Variables. **Biometrika**. V. 54, p. 167–179, 1967.

148. WANG, H., ZHANG, L., YIN, K., LUO, H., LI, J. Landslide identification using machine learning. **Geoscience Frontiers**. V. 12, p. 351–364, 2021. DOI: 10.1016/j.gsf.2020.02.012

149. WANG, Y., FANG, Z., WANG, M., PENG, L., HONG, H. Comparative study of landslide susceptibility mapping with different recurrent neural networks. **Computers & Geosciences**. V. 138, 18p., 2020. DOI: 10.1016/j.cageo.2020.104445

150. XU, B., WANG, N., CHEN, T., LI, M. Empirical Evaluation of Rectified Activations in Convolutional Network. **ArXiv preprint**. 5p., 2015. DOI: 10.48550/arXiv.1505.00853

151. XU, C., XU, X., DAI, F., WU, Z., HE, H., SHI, F., WU, X., XU, S. Application of an incomplete landslide inventory, logistic regression model and its validation for landslide susceptibility mapping related to the May 12, 2008 Wenchuan earthquake of China. **Natural Hazards**. V. 68, p. 883–900, 2013. DOI: 10.1007/s11069-013-0661-7

152. YESILNACAR, E., SÜZEN, M.L. A land-cover classification for landslide susceptibility mapping by using feature components. **International Journal of Remote Sensing**. V. 27, p. 253–275, 2006. DOI: 10.1080/0143116050030042

153. YI, Y., ZHANG, W., XU, X., ZHANG, Z., WU, X. Evaluation of neural network models for landslide susceptibility assessment. **International Journal of Digital Earth**. V. 15, p. 934–953, 2022. DOI: 10.1080/17538947.2022.2062467

154. YI, Y., ZHANG, Z., ZHANG, W., XU, C. Comparison of Different Machine Learning Models For Landslide Susceptibility Mapping. In: International Geoscience and Remote Sensing Symposium, 2019, Yokohama, Japão. **Proceedings…** Nova York: IEEE Press. 2019. p. 9318–9321. DOI: 10.1109/IGARSS.2019.8898208

155. YILMAZ, I. A case study from Koyulhisar (Sivas-Turkey) for landslide susceptibility mapping by artificial neural networks. **Bulletin of Engineering Geology and the Environment**. V. 68, p. 297–306, 2009. DOI: 10.1007/s10064-009-0185-2

156. YOUSSEF, A.M., POURGHASEMI, H.R. Landslide susceptibility mapping using machine learning algorithms and comparison of their performance at Abha Basin, Asir Region, Saudi Arabia. **Geoscience Frontiers**. V. 12, p. 639–655, 2021. DOI: 10.1016/j.gsf.2020.05.010

157. ZAJMI, L., AHMED, F.Y.H., JAHARADAK, A.A. Concepts, Methods, and Performances of Particle Swarm Optimization, Backpropagation, and Neural Networks. **Applied Computational Intelligence and Soft Computing**. V. 2018, 7p., 2018. DOI: 10.1155/2018/9547212

158. ZHANG, K., WU, X., NIU, R., YANG, K., ZHAO, L. The assessment of landslide susceptibility mapping using random forest and decision tree methods in the Three Gorges Reservoir area, China. **Environmental Earth Sciences**. V. 76, n. 405, 20p., 2017. DOI: 10.1007/s12665-017-6731-5

159. ZHANG, S., BAI, L., LI, Y., LI, W., XIE, M. Comparing Convolutional Neural Network and Machine Learning Models in Landslide Susceptibility Mapping: A Case Study in Wenchuan County. **Frontiers in Environmental Science**. V. 10, 12p., 2022. DOI: 10.3389/fenvs.2022.886841

160. ZIMMERMANN, M., BICHSEL, M., KIENHOLZ, H. Mountain Hazards Mapping in the Khumbu Himal, Nepal. **Mountain Research and Development**. V. 6, n. 1, p. 29–40, 1986. DOI: 10.2307/3673338